ARTIFICIAL VISCOSITY TO GET BOTH ROBUSTNESS AND DISCRETE ENTROPY INEQUALITIES

CHRISTOPHE BERTHON*, MANUEL J. CASTRO DíAZ†, ARNAUD DURAN‡, TOMÁS MORALES DE LUNA§, AND KHALED SALEH‡

AMS subject classifications. 65M08, 65M12

Key words. Evolution laws, finite volume schemes, CFL-like condition, robustness, discrete entropy inequalities.

Abstract. In the present work, we consider the numerical approximation of the weak solutions of first-order system of evolution laws supplemented with entropy inequalities. The systems under consideration are hyperbolic as soon as a conservation form is satisfied, but such stability property may be lost for non-conservative systems. Here, we show that the robustness and the entropy stability of any finite volume numerical scheme can be restored by introducing a suitable artificial numerical viscosity.

1. Introduction. The present work concerns the stability of numerical schemes to approximate the weak solutions of a $N \times N$ evolution law systems in the following form:

$$\partial_t w + \partial_x f(w) + A(w)\partial_x w = 0, \qquad x \in \mathbb{R}, \quad t > 0, \tag{1.1}$$

where $(x,t) \in \mathbb{R}^+ \times \mathbb{R} \mapsto w(x,t)$ denotes the unknown vector assumed to belong to an open set $\Omega \in \mathbb{R}^N$. Here, $f : \Omega \to \mathbb{R}^N$ is a smooth enough flux function and $A : \Omega \to \mathbb{R}^N \times \mathbb{R}^N$ denotes a given smooth matrix. From now on, it is worth noticing that we do not impose the matrix $\nabla_w f(w) + A(w)$ to be diagonalizable in $\mathbb{R}$. As a consequence, in this work, the system (1.1) is not necessarily hyperbolic over Ω.

Now, an important assumption must be put on the exact Riemann solutions of (1.1), denoted $\mathcal{W}_{ex}\left(\frac{x}{t}; w_L, w_R\right)$, for an initial data given by

$$w_0(x) = \begin{cases} w_L, & \text{if } x < 0, \\ w_R, & \text{if } x > 0, \end{cases}$$

where w_L and w_R are two given constant states in Ω. Indeed, we assume the existence of $\lambda^\star > 0$ such that the exact Riemann solution is in the form

$$\begin{aligned} \mathcal{W}_{ex}\left(\frac{x}{t}; w_L, w_R\right) &= w_L \qquad \text{for all } x < -\lambda^\star t, \\ \mathcal{W}_{ex}\left(\frac{x}{t}; w_L, w_R\right) &= w_R \qquad \text{for all } x > \lambda^\star t. \end{aligned} \tag{1.2}$$

In fact, such an assumption is immediately satisfied by any hyperbolic system of conservation laws and it is, in general, assumed for non-conservative systems with real or complex eigenvalues.

*Université de Nantes, CNRS UMR 6629, Laboratoire de Mathématiques Jean Leray, 2 rue de la Houssinière, BP 92208, 44322 Nantes, France.

†Departamento de Análisis Matemático, Estadística e Investigación Operativa, y Matemática Aplicada, Universidad de Málaga, Campus de Teatinos s/n, Málaga 29080, Spain.

‡Institut Camille Jordan, CNRS UMR 5208, Université Claude Bernard Lyon 1, 43 boulevard du 11 novembre 1918, F-69622 Villeurbanne Cedex, France.

§Departamento de Matemáticas, Universidad de Córdoba, Campus de Rabanales, 14071 Córdoba, Spain.

In addition, we assume the system (1.1) to be endowed with an entropy inequality given by

$$\partial_t \eta(w) + \partial_x G(w) \leq 0, \qquad \text{in the weak sense,} \tag{1.3}$$

where the entropy function $\eta : \Omega \to \mathbb{R}$ is convex and the entropy flux function $G : \Omega \to \mathbb{R}$ is defined by $\nabla_w G(w) = \nabla_w \eta(w) \cdot (\nabla_w f(w) + A(w))$. We recall that the existence of entropy inequalities is strongly related to the hyperbolicity of the system as long as (1.1) is in conservation form, namely $A \equiv 0$. However, by adopting a non-conservative system, with $A \not\equiv 0$, the system (1.1) may simultaneously get eigenvalues in $\mathbb{C}$ and admit entropy inequalities.

These entropy inequalities are essential to correctly define the discontinuous shock solutions (see [35, 44, 54, 55, 70]) as long as (1.1) is given in conservation form. Now, after [10, 22, 36, 50, 57], it is well-known that entropy inequalities, in general, are not sufficient to suitably define shock waves as long as the matrix $\nabla_w f(w) + A(w)$ never recasts as a Jacobian matrix. Indeed, because of the non-conservative product $A(w)\partial_x w$, the system (1.1) presents a major difficulty because the discontinuous solutions have no sense in the distributional framework. However, to give a sense to the weak solutions, Dal Maso, LeFLoch and Murat [36] have introduced a suitable theory, the so-called path-theory, to exhibit the existence of the entropy weak solutions for system in non-conservative form (see [56, 58]). In addition, we mention that the entropy inequalities are fully natural when considering viscous approach to characterize the Riemann solution of hyperbolic systems in non-conservative form (for instance, see [10, 29]).

Now, for both conservative and non-conservative systems, the entropy inequalities produce important estimations to be replaced by: since we get $\int_{\mathbb{R}} \eta(w(x,t))dx \leq \int_{\mathbb{R}} \eta(w_0(x))dx$, we obtain, in a sense to be prescribed, a weighted$-L^2$ estimation of w for all $t > 0$. Moreover, according to [10, 29], the entropy inequality (1.3) enforced an additional control of the discontinuous solutions. Indeed, across a discontinuity separating two constant states w_L and w_R and propagating with a velocity σ,from (1.3) we have $-\sigma(\eta(w_R) - \eta(w_L)) + (G(w_R) - G(w_L)) \leq 0$. Because of the natural conservation form of (1.3), let us mention that the above entropy definition is free from the selected path for systems in non-conservative form. Put in other words, according to [36], a shock discontinuity depends on a path ϕ to get $(w_L^\phi, w_R^\phi; \sigma^\phi)$. But all the possible shocks, according to the choice of the path ϕ, satisfy the local entropy inequality $-\sigma^\phi(\eta(w_R^\phi) - \eta(w_L^\phi)) + (G(w_R^\phi) - G(w_L^\phi)) \leq 0$. At this level, it is thus essential to understand that the entropy inequality (1.3) does not solve the well-known non-conservative product ambiguity but gives suitable estimations.

During the last half century, numerous numerical schemes have been designed to approximate the weak solutions of (1.1). Clearly, it is not possible to give an exhaustive bibliography, but the reader is referred to the pioneer work by Parés [65] where a path-consistent scheme is derived in order to produce relevant approximations of the weak solutions of (1.1) according to the path-theory [36] (see also [24, 43, 44, 47, 53, 57, 61, 76] and references therein for a review about the numerical approximation of hyperbolic systems of conservation laws, balance laws and hyperbolic non-conservative systems). In the present work, we focus our attention on the well-known 3-point finite

volume explicit schemes. These numerical techniques read

$$w_i^{n+1} = w_i^n - \frac{\Delta t}{\Delta x}\left(f_\Delta(w_i^n, w_{i+1}^n) - f_\Delta(w_{i-1}^n, w_i^n)\right) - \frac{\Delta t}{2\Delta x}\left(A_\Delta^L(w_i^n, w_{i+1}^n)\cdot(w_{i+1}^n - w_i^n) + A_\Delta^R(w_{i-1}^n, w_i^n)\cdot(w_i^n - w_{i-1}^n)\right), \tag{1.4}$$

where $f_\Delta : \Omega \times \Omega \to \mathbb{R}^N$ denotes the Lipschitz-continuous numerical flux function such that $f_\Delta(w,w) = f(w)$ for all w in Ω. Moreover, $A_\Delta^{L,R} : \Omega \times \Omega \to \mathbb{R}^N \times \mathbb{R}^N$ is a matrix consistent with $A(\cdot)$, namely $A_\Delta^{L,R}(w,w) = A(w)$. Here, w_i^n approximates $w(x,t)$ for all x in a cell $(x_{i-\frac{1}{2}}, x_{i+\frac{1}{2}})$ of size Δx at time t^n. For the sake of simplicity in the forthcoming developments, both space and time increments Δx and Δt are constant, and we set $x_i = (x_{i-\frac{1}{2}} + x_{i+\frac{1}{2}})/2$ the middle of the cell $(x_{i-\frac{1}{2}}, x_{i+\frac{1}{2}})$. We underline that the definition of f_Δ and $A_\Delta^{L,R}$ are free and the reader may refer to any scheme derivation proposed in the literature.

Now, equipped with these numerical approximations, three natural questions arise:

1. How is the time increment Δt restricted?
2. Do the updated states $(w_i^{n+1})_{i\in\mathbb{Z}}$ be in Ω as soon as $w_i^n \in \Omega$ for all $i \in \mathbb{Z}$?
3. How can we restore, at the numerical level, an entropy inequality (1.3)?

Concerning the first question, the well-known CFL restriction produces an interesting response. Indeed, after [78], stability criterion can be imposed as follows:

$$\frac{\Delta t}{\Delta x}\max_{i\in\mathbb{Z},\ 1\le\ell\le N}|\lambda_\ell(w_i^n)| \le \frac{1}{2}, \tag{1.5}$$

where $(\lambda_\ell(w))_{1\le\ell\le N}$ denote the eigenvalues of the matrix $\nabla_w f(w) + A(w)$. According to the definition of $f_\Delta(\cdot,\cdot)$ and $A_\Delta^{L,R}(\cdot,\cdot)$, such a time restriction may be insufficient to ensure a stability condition in a sense to be prescribed. Moreover, in (1.5), the eigenvalues are expected to be real. As a consequence, it is worth noticing that the CFL-like condition (1.5) is suitable for hyperbolic systems with explicit eigenvalues. Unfortunately, systems issuing from sophisticated physics do not necessarily admit real eigenvalues. For instance, let us consider the bi-layer shallow water model [20–23, 27,28] or sediment transport model [26,34,46,64] for which the associated eigenvalues do not have an explicit simple expression and belong to $\mathbb{R}$ or $\mathbb{C}$.

Next, concerning the second question, this problem is frequently called realizability or robustness of the scheme. This issue is, in general, tackled in the derivation of a new scheme. Indeed, if the numerical robustness is lost, no longer the existence of the numerical approximation can be ensured. As a consequence, the robustness (or realizability) must be preserved to validate a scheme.

Finally, concerning the last question, the derivation of discrete entropy inequalities remains a very difficult task. Indeed, to enforce the required entropy stability, the updated states $(w_i^{n+1})_{i\in\mathbb{Z}}$, given by (1.4), are expected to satisfy for all $i \in \mathbb{Z}$

$$\eta(w_i^{n+1}) \le \eta(w_i^n) - \frac{\Delta t}{\Delta x}\left(G_\Delta(w_i^n, w_{i+1}^n) - G_\Delta(w_{i-1}^n, w_i^n)\right), \tag{1.6}$$

where $G_\Delta(\cdot,\cdot)$ is a numerical entropy flux function such that $G_\Delta(w,w) = G(w)$ for all w in Ω. As long as $N \ge 2$, up to our knowledge, very few schemes are entropy preserving and satisfy a discrete entropy inequality in the form (1.6). The original Godunov scheme [45] (see also [44,76]) and the HLL scheme [48] are proved to be entropy preserving. The establishment of this stability property comes from the entropy

inequality (1.3) satisfied by the exact solution. Some kinetic schemes [15,52] and relaxation schemes [17–19,30,33], including the well-known HLLC scheme [17,77], are also proved to preserve the entropy stability, by adopting some convex minimization principles. Several works propose more general conditions to get the expected discrete entropy inequalities when considering conservative hyperbolic systems. For instance, in [48], the authors introduce a local entropy condition per interface. Excepted for the Godunov scheme and the one-intermediate state HLL scheme (see also [11]), this condition is hardly reachable. We also mention the important work by Tadmor [74,75] where, arguing the entropy variables, discrete entropy inequalities (1.6) are derived according to a suitable control of the numerical viscosity. We also refer to the work by Bouchut [16] where the discrete entropy inequalities (1.6) are obtained for hyperbolic system of conservation laws by arguing a suitable kinetic reformulation. In fact, most of the designed schemes perform good approximations, without spurious numerical perturbations, so that they are certainly entropy preserving but the establishment of the required entropy stability is not reachable. However, it is important to notice that several schemes are entropy violating (for instance, see [38,39,62,68]) and may capture wrong shock solutions. In the literature [37,49], entropy corrections have been introduced but fully discrete entropy inequalities (1.6) are, in general, not established (see also [1,3,6]). From now on, as soon as $A(.) \not\equiv 0$ in (1.1), we emphasize that the well known non-conservative product ambiguity [36] is here not solved. According to [5,9,22,50], an approximated shock solution may depend on the selected numerical scheme; namely a dependence on the choice of of $f_\Delta(.,.)$, $A^L_\Delta(.,.)$ and $A^R_\Delta(.,.)$. Since the entropy inequality (1.3) does not solve the non-conservative product ambiguity, it is worth noticing that the existence of a discrete entropy inequality never ensures the convergence to the expected weak solution according to a selected path, at the discrepancy of conservative systems with $A(.) \equiv 0$. As underline in [22,50] (see also [4]), as soon as $A(.) \not\equiv 0$ the approximate solution converges to a weak solution of (1.1) up to a measure. Let us notice that a discrete entropy inequality cannot suitably control such a wrong measure but gives a suitable L^2 control of the approximated solution.

In order to overcome the difficulty of the convergence towards the correct solution, one could use viscosity-free methods based on Random Choice (see [32,41,42]), front-tracking methods (see [40,67]) or methods based on a proper in-cell discontinuous reconstruction (see [31,66]) ; or controlled viscosity methods based on the equivalent equation (see [8,51]); or use methods that control the entropy losses across discontinuities like nonlinear projection methods (see [14]); or methods based on kinetic relations (see [10,60]), etc. The interested reader is referred to [59] and the references therein for a detailed discussion on this topic.
Let us mention that, even in the case in which jump relations are explicitly given by the physics of the problem, the design of numerical methods converging to the correct weak solutions is still challenging: this is the case for the Kapila multiphase model that has been discretized in [7] by a numerical method that is a hybridization of Roe and Glimm schemes. Recent approaches to construct numerical methods that converge to the correct weak solution for the non-conservative formulation of the pressure based Euler equations can found in [2].

In the present work, we address the three asked questions by adopting artificial viscosity. Following ideas introduced by Tadmor [71,73–75], and its generalization to non-conservative systems in [25], the numerical viscosity is a essential tool to recover the required entropy estimation (1.6). As a consequence, the scheme improved by

artificial viscosity under consideration is here given by

$$\begin{aligned} w_i^{n+1} = w_i^n &- \frac{\Delta t}{\Delta x}\left(f_\Delta(w_i^n, w_{i+1}^n) - f_\Delta(w_{i-1}^n, w_i^n)\right) \\ &- \frac{\Delta t}{2\Delta x}\left(A_\Delta^L(w_i^n, w_{i+1}^n)\cdot(w_{i+1}^n - w_i^n) + A_\Delta^R(w_{i-1}^n, w_i^n)\cdot(w_i^n - w_{i-1}^n)\right) \\ &+ \frac{\gamma}{2}\frac{\Delta t}{\Delta x}\left(w_{i+1}^n - 2w_i^n + w_{i-1}^n\right), \end{aligned} \tag{1.7}$$

where $\gamma \geq 0$ is a parameter to be fixed according to the expected stability properties. To judiciously control γ, we here suggest to derive a local Godunov-type reformulation [12, 13, 48]. We adopt the local integral consistency stated by Harten, Lax and van Leer [48, Theorem 3.1] to get the required control of the artificial viscosity and to obtain the expected estimation (1.6) in the same spirit of Tadmor in [74] and its generalization to non-conservative systems [25] . Moreover, this control of the artificial viscosity comes with a relevant restriction of the time increment Δt by exhibiting a CFL-like criterion. In fact, the local Godunov-type reformulation of the scheme (1.4) also leads to a condition to enforce the updated state w_i^{n+1} to belong to Ω. This condition is, once again, controlled by the artificial viscosity.

The present paper is organized as follows. In the next section, we present local Godunov-type reformulations [12, 13, 48] and the introduction of judicious approximate Riemann solvers. We also give assumptions to be satisfied by the exact Riemann solution for (1.1) in order to state our main result where we show a suitable CFL condition to get the expected robustness and the discrete entropy inequalities. Next, Section 3 and Section 4 are devoted to the establishment of the main result. Both robustness (Section 3) and discrete entropy inequalities (Section 4) are obtained by involving a relevant Godunov-type reformulation. The last section is devoted to numerical experiments in order to illustrate the relevance of the proposed stability enforcing technique. First, we perform numerical approximations of the solutions of the isentropic gas dynamic model and the shallow water model. We show the ability of the here designed technique to stabilize entropy violating schemes. Next, we consider the bi-layer shallow-water model. Because the eigenvalues of the model remain unknown, the interest of the stabilizing technique is twofold since, in addition to both robustness and entropy preserving properties, we obtain a natural CFL-like condition.

2. Godunov-type reformulation and main results. We here reformulate the viscous scheme (1.7) as a Godunov-type scheme. We address the reader to [24] and the references therein for further detail. To do so, we first introduce an approximate Riemann solver as follows:

$$\bar{\mathcal{W}}^{\mathcal{R}}\left(\frac{x}{t}; w_i^n, w_{i+1}^n\right) = \begin{cases} w_i^n, & \text{if } x < -(\lambda_{i+\frac{1}{2}} + \gamma)t, \\ \bar{w}_{i+\frac{1}{2}}, & \text{if } -(\lambda_{i+\frac{1}{2}} + \gamma)t < x < -\lambda_{i+\frac{1}{2}}t, \\ w_{i+\frac{1}{2}}^{L\star}, & \text{if } -\lambda_{i+\frac{1}{2}}t < x < 0, \\ w_{i+\frac{1}{2}}^{R\star}, & \text{if } 0 < x < \lambda_{i+\frac{1}{2}}t, \\ \bar{w}_{i+\frac{1}{2}}, & \text{if } \lambda_{i+\frac{1}{2}}t < x < (\lambda_{i+\frac{1}{2}} + \gamma)t, \\ w_{i+1}^n, & \text{if } x > (\lambda_{i+\frac{1}{2}} + \gamma)t, \end{cases} \tag{2.1}$$

where $w_{i+\frac{1}{2}}^{L\star}$ and $w_{i+\frac{1}{2}}^{R\star}$ are defined by

$$w_{i+\frac{1}{2}}^{L\star} = w_i^n - \frac{1}{\lambda_{i+\frac{1}{2}}}\left(f_\Delta(w_i^n, w_{i+1}^n) - f(w_i^n)\right) - \frac{1}{2\lambda_{i+\frac{1}{2}}} A_\Delta^L(w_i^n, w_{i+1}^n)\cdot(w_{i+1}^n - w_i^n), \tag{2.2}$$

$$w_{i+\frac{1}{2}}^{R\star} = w_{i+1}^n + \frac{1}{\lambda_{i+\frac{1}{2}}}\left(f_\Delta(w_i^n, w_{i+1}^n) - f(w_{i+1}^n)\right) - \frac{1}{2\lambda_{i+\frac{1}{2}}} A_\Delta^R(w_i^n, w_{i+1}^n)\cdot(w_{i+1}^n - w_i^n), \tag{2.3}$$

where we have set

$$\bar{w}_{i+\frac{1}{2}} = \frac{1}{2}(w_i^n + w_{i+1}^n). \tag{2.4}$$

At this level, the wave speed parameter $\lambda_{i+\frac{1}{2}}$ is only imposed to be positive but it must be selected according to forthcoming stability conditions.

Now, we are able to exhibit the expected Godunov-type reformulation.

LEMMA 2.1. *Under the CFL-like condition*

$$\frac{\Delta t}{\Delta x}\max_{i\in\mathbb{Z}}\left(\lambda_{i+\frac{1}{2}} + \gamma\right) \le \frac{1}{2}, \tag{2.5}$$

the viscous scheme (1.7) equivalently reformulates as follows:

$$\begin{aligned} w_i^{n+1} =& \frac{1}{\Delta x}\int_{x_{i-\frac{1}{2}}}^{x_i} \bar{\mathcal{W}}^{\mathcal{R}}\left(\frac{x - x_{i-\frac{1}{2}}}{\Delta t}; w_{i-1}^n, w_i^n\right) dx \\ &+ \frac{1}{\Delta x}\int_{x_i}^{x_{i+\frac{1}{2}}} \bar{\mathcal{W}}^{\mathcal{R}}\left(\frac{x - x_{i+\frac{1}{2}}}{\Delta t}; w_i^n, w_{i+1}^n\right) dx. \end{aligned} \tag{2.6}$$

From now on, let us remark that, as soon as $\gamma = 0$, the intermediate states $\bar{w}_{i+\frac{1}{2}}$ no longer appear within the approximate Riemann solver (2.1) so that the Godunov-type reformulation (2.6) coincides with the original scheme (1.4). Moreover, we emphasize that the artificial viscosity involved in (1.7) is entirely contained in the two intermediate states given by $\bar{w}_{i+\frac{1}{2}}$. Such a splitting within the intermediate states will allow to control the entropy dissipation rate issuing from the artificial viscosity independently from the entropy dissipation rate of the initial scheme (1.4). Moreover, it is important to notice that this splitting results from the introduction of the free parameter $\lambda_{i+\frac{1}{2}} > 0$. In fact, to establish the entropy preserving property, a lower bound of $\lambda_{i+\frac{1}{2}}$ will be exhibited.

Now, we establish the scheme reformulation stated Lemma 2.1.

Proof. Direct computations give the following sequence of equalities:

$$\begin{aligned} \frac{1}{\Delta x}\int_{x_{i-\frac{1}{2}}}^{x_i} \bar{\mathcal{W}}^{\mathcal{R}}\left(\frac{x - x_{i-\frac{1}{2}}}{\Delta t}; w_{i-1}^n, w_i^n\right) dx &= \frac{1}{\Delta x}\int_0^{\Delta x/2} \bar{\mathcal{W}}^{\mathcal{R}}\left(\frac{x}{\Delta t}; w_{i-1}^n, w_i^n\right) dx, \\ &= \frac{1}{2}w_i^n + \gamma\frac{\Delta t}{\Delta x}(\bar{w}_{i-\frac{1}{2}} - w_i^n) + \lambda_{i-\frac{1}{2}}\frac{\Delta t}{\Delta x}(w_{i-\frac{1}{2}}^{R\star} - w_i^n), \\ \frac{1}{\Delta x}\int_{x_i}^{x_{i+\frac{1}{2}}} \bar{\mathcal{W}}^{\mathcal{R}}\left(\frac{x - x_{i+\frac{1}{2}}}{\Delta t}; w_i^n, w_{i+1}^n\right) dx &= \frac{1}{\Delta x}\int_{-\Delta x/2}^0 \bar{\mathcal{W}}^{\mathcal{R}}\left(\frac{x}{\Delta t}; w_i^n, w_{i+1}^n\right) dx, \\ &= \frac{1}{2}w_i^n + \gamma\frac{\Delta t}{\Delta x}(\bar{w}_{i+\frac{1}{2}} - w_i^n) + \lambda_{i+\frac{1}{2}}\frac{\Delta t}{\Delta x}(w_{i+\frac{1}{2}}^{L\star} - w_i^n). \end{aligned}$$

Arguing the definition of the intermediate states, given by (2.2), (2.3) and (2.4), the updated state w_i^{n+1}, defined by (1.7), rewrites as follows:

$$w_i^{n+1} = \frac{1}{\Delta x}\int_0^{\frac{\Delta x}{2}} \bar{\mathcal{W}}^{\mathcal{R}}\left(\frac{x}{\Delta t}; w_{i-1}^n, w_i^n\right)\, dx + \frac{1}{\Delta x}\int_{-\frac{\Delta x}{2}}^{0} \bar{\mathcal{W}}^{\mathcal{R}}\left(\frac{x}{\Delta t}; w_i^n, w_{i+1}^n\right)\, dx.$$

Next, under the CFL restriction (2.5), two successive approximate Riemann solver, namely $\bar{\mathcal{W}}^{\mathcal{R}}\left(\frac{x-x_{i-\frac{1}{2}}}{\Delta t}; w_{i-1}^n, w_i^n\right)$ and $\bar{\mathcal{W}}^{\mathcal{R}}\left(\frac{x-x_{i+\frac{1}{2}}}{\Delta t}; w_i^n, w_{i+1}^n\right)$, never interact. As a consequence, the expected reformulation (2.6) is obtained by a change of variable in the integrals. The proof is thus completed. □

In fact, the Godunov-type reformulation is not unique. It will be convenient to present a second reformulation based on the following approximate Riemann solver:

$$\widetilde{\mathcal{W}}^{\mathcal{R}}\left(\frac{x}{t}; w_i^n, w_{i+1}^n\right) = \begin{cases} w_i^n, & \text{if } x < -(\lambda_{i+\frac{1}{2}} + \gamma)t, \\ \widetilde{w}_{i+\frac{1}{2}}^{L\star}, & \text{if } -(\lambda_{i+\frac{1}{2}} + \gamma)t < x < 0, \\ \widetilde{w}_{i+\frac{1}{2}}^{R\star}, & \text{if } 0 < x < (\lambda_{i+\frac{1}{2}} + \gamma)t, \\ w_{i+1}^n, & \text{if } x > (\lambda_{i+\frac{1}{2}} + \gamma)t, \end{cases} \tag{2.7}$$

where

$$\widetilde{w}_{i+\frac{1}{2}}^{L\star} = \left(1 - \frac{\lambda_{i+\frac{1}{2}}}{\lambda_{i+\frac{1}{2}} + \gamma}\right)\bar{w}_{i+\frac{1}{2}} + \frac{\lambda_{i+\frac{1}{2}}}{\lambda_{i+\frac{1}{2}} + \gamma} w_{i+\frac{1}{2}}^{L\star}, \tag{2.8}$$

$$\widetilde{w}_{i+\frac{1}{2}}^{R\star} = \left(1 - \frac{\lambda_{i+\frac{1}{2}}}{\lambda_{i+\frac{1}{2}} + \gamma}\right)\bar{w}_{i+\frac{1}{2}} + \frac{\lambda_{i+\frac{1}{2}}}{\lambda_{i+\frac{1}{2}} + \gamma} w_{i+\frac{1}{2}}^{R\star}. \tag{2.9}$$

Equipped with this second approximate Riemann solver, we now give a new equivalent Godunov-type reformulation.

Lemma 2.2. *Under the CFL-like condition (2.5), the viscous scheme (1.7) equivalently reformulates as follows:*

$$\begin{aligned} w_i^{n+1} =& \frac{1}{\Delta x}\int_{x_{i-\frac{1}{2}}}^{x_i} \widetilde{\mathcal{W}}^{\mathcal{R}}\left(\frac{x - x_{i-\frac{1}{2}}}{\Delta t}; w_{i-1}^n, w_i^n\right)\, dx \\ &+ \frac{1}{\Delta x}\int_{x_i}^{x_{i+\frac{1}{2}}} \widetilde{\mathcal{W}}^{\mathcal{R}}\left(\frac{x - x_{i+\frac{1}{2}}}{\Delta t}; w_i^n, w_{i+1}^n\right)\, dx. \end{aligned} \tag{2.10}$$

The establishment of the above result is similar to Lemma 2.1 and the proof is left to the reader.

We are now able to state our main result where we claim that the viscous scheme (1.7) is robust and entropy satisfying as soon as $\lambda_{i+\frac{1}{2}}$ and γ are fixed large enough.

Theorem 2.3. *Let $(w_i^n)_{i\in\mathbb{Z}}$ be given in Ω. Let w_i^{n+1} be given by the viscous scheme (1.7). Assume that*

$$\begin{aligned} &\frac{1}{2}\left(A_\Delta^L(w_i^n, w_{i+1}^n) + A_\Delta^R(w_i^n, w_{i+1}^n)\right)\cdot(w_{i+1}^n - w_i^n) = \\ &\qquad \frac{1}{\Delta t}\int_0^{\Delta t}\int_{-\lambda_{i+\frac{1}{2}}\Delta t}^{\lambda_{i+\frac{1}{2}}\Delta t} A\left(\mathcal{W}_{ex}\left(\frac{x}{t}; w_i^n, w_{i+1}^n\right)\right)\partial_x \mathcal{W}_{ex}\left(\frac{x}{t}; w_i^n, w_{i+1}^n\right)\, dx\, dt, \end{aligned} \tag{2.11}$$

Let $\lambda_{i+\frac{1}{2}} > \lambda^\star$. Let us set

$$\mathcal{E}^0_{i+\frac{1}{2}} = \lambda_{i+\frac{1}{2}} \left(\eta(w^{L\star}_{i+\frac{1}{2}}) + \eta(w^{R\star}_{i+\frac{1}{2}}) - \eta(w^n_i) - \eta(w^n_{i+1}) \right) + \left(G(w^n_{i+1}) - G(w^n_i) \right), \tag{2.12}$$

$$\mathcal{D}_{i+\frac{1}{2}} = 2\eta(\bar{w}_{i+\frac{1}{2}}) - \eta(w^n_i) - \eta(w^n_{i+1}), \tag{2.13}$$

and define γ as follows:

$$\gamma = \max_{i\in\mathbb{Z}} \left(0, -\frac{\mathcal{E}^0_{i+\frac{1}{2}}}{\mathcal{D}_{i+\frac{1}{2}}} \right). \tag{2.14}$$

Let Δt be restricted by the CFL-like condition (2.5). Assume that the Hessian matrix $\nabla^2_w \eta(w)$ is positive definite. Then $\gamma \geq 0$ is bounded and the viscous scheme (1.7) is

1. *robust: $w^{n+1}_i \in \Omega$, as long as γ satisfies in addition*

$$\gamma \geq \max \left\{ \frac{\lambda_{i+\frac{1}{2}}}{r_{i+\frac{1}{2}}} \left\| w^{L\star}_{i+\frac{1}{2}} - \bar{w}_{i+\frac{1}{2}} \right\| - \lambda_{i+\frac{1}{2}}, \frac{\lambda_{i+\frac{1}{2}}}{r_{i+\frac{1}{2}}} \left\| w^{R\star}_{i+\frac{1}{2}} - \bar{w}_{i+\frac{1}{2}} \right\| - \lambda_{i+\frac{1}{2}} \right\}, \tag{2.15}$$

   where $r_{i+\frac{1}{2}} > 0$ is such that the ball $B(\bar{w}_{i+\frac{1}{2}}, r_{i+\frac{1}{2}})$ centered on $\bar{w}_{i+\frac{1}{2}}$ with radius $r_{i+\frac{1}{2}}$ is entirely contained within Ω.

2. *entropy preserving: w^{n+1}_i verifies the discrete entropy inequality (1.6).*

The proof of this statement is the purpose of the two next sections. Before going any further, it should be noted that γ given by condition (2.14) is bounded. An estimate of this bound will be given later in the proof of Lemma (see estimate (4.5)). At the practical level, γ is computed as the maximum in (2.14) and (2.15) at the beginning of each time step and the time increment Δt is defined according to (2.5) afterwards. To conclude this section, let us comment the assumptions imposed in the above result. First, by enforcing $\lambda_{i+\frac{1}{2}}$ to be large enough is a very natural assumption. Formally, the condition $\lambda_{i+\frac{1}{2}} > \lambda^\star$ can be found in [48]. Indeed, as long as the eigenvalues $(\lambda_\ell(w))_{1\leq\ell\leq N}$ of the matrix $\nabla_w f(w) + A(w)$ are known, the assumption stated on $\lambda_{i+\frac{1}{2}}$ reads

$$\lambda_{i+\frac{1}{2}} \geq \max_{1\leq\ell\leq N} \left(|\lambda_\ell(w^n_i)|, |\lambda_\ell(w^n_{i+1})| \right).$$

As a consequence, this parameter cannot be as small as we want and that is coherent with the CFL-like restriction (2.5). Next, we emphasize that the assumption (2.11) only concerns systems (1.1) in non-conservative form [22, 23, 26, 27, 65]. In addition, let us mention that the entropies issuing from problems of physical interest admit, in general, a positive definite Hessian matrix.

3. Artificial viscosity and robustness. In this section, we show that the artificial viscosity may enforce the robustness of the numerical scheme.

LEMMA 3.1. *Assume Ω is convex. Let $(w^n_i)_{i\in\mathbb{Z}}$ be a given sequence in Ω. Let w^{n+1}_i be given by the viscous scheme (2.6). Let Δt be restricted according to the CFL-like condition (2.5). As soon as $\gamma \geq 0$ is large enough according to (2.15), then $w^{n+1}_i \in \Omega$ for all $i \in \mathbb{Z}$.*

Proof. Since Ω is convex, in view of (2.10) and thanks to the CFL condition (2.5), it is sufficient to prove that $\widetilde{w}^{L\star}_{i+\frac{1}{2}}, \widetilde{w}^{R\star}_{i+\frac{1}{2}} \in \Omega$ whenever $w^n_i, w^n_{i+1} \in \Omega$.

Now, clearly the intermediate state $\bar{w}_{i+\frac{1}{2}}$, given by (2.4), stays in Ω. Moreover, since Ω is an open set, then there exists $r_{i+\frac{1}{2}} > 0$ such that

$$w \in \Omega \text{ for every } w \text{ satisfying } \left\| w - \bar{w}_{i+\frac{1}{2}} \right\| < r_{i+\frac{1}{2}}.$$

Therefore, it is a sufficient condition to have

$$\left\| \widetilde{w}^{L\star}_{i+\frac{1}{2}} - \bar{w}_{i+\frac{1}{2}} \right\| = \frac{\lambda_{i+\frac{1}{2}}}{\lambda_{i+\frac{1}{2}} + \gamma} \left\| w^{L\star}_{i+\frac{1}{2}} - \bar{w}_{i+\frac{1}{2}} \right\| < r_{i+\frac{1}{2}},$$

$$\left\| \widetilde{w}^{R\star}_{i+\frac{1}{2}} - \bar{w}_{i+\frac{1}{2}} \right\| = \frac{\lambda_{i+\frac{1}{2}}}{\lambda_{i+\frac{1}{2}} + \gamma} \left\| w^{R\star}_{i+\frac{1}{2}} - \bar{w}_{i+\frac{1}{2}} \right\| < r_{i+\frac{1}{2}},$$

where $w^{L\star}_{i+\frac{1}{2}}$ and $w^{R\star}_{i+\frac{1}{2}}$, defined by (2.8) and (2.9), do not depend on γ. As a consequence, the condition (2.15) immediately imposes $\widetilde{w}^{L\star}_{i+\frac{1}{2}}$ and $\widetilde{w}^{R\star}_{i+\frac{1}{2}}$ to belong to Ω and the proof is achieved. □

Let us emphasize that the admissible states, here, belong to an open set. According to some particular physics, Ω is not necessarily open (for instance, see the shallow-water model [12, 17, 63]). The transition from states in Ω to states in $\partial\Omega$, in general, needs a specific attention and it is not considered in the present work.

In addition to this general result, a constructive method can be proposed in the particular case where Ω is of the form:

$$\Omega = \left\{ w \in \mathbb{R}^d \, , \, p_j(w) > 0 \, , \, j = 1 \, , \cdots \, , L \right\} \, , \tag{3.1}$$

where $(p_j)_{j=1\,,\cdots,L}$ are smooth functions. According to the convexity of Ω, we recall that a sufficient condition to have robustness is to enforce the quantities (2.8), (2.9) to belong to Ω, which means that $p_j(\widetilde{w}^{L,*}_{i+1/2}) > 0$ and $p_j(\widetilde{w}^{R,*}_{i+1/2}) > 0$ for $j = 1 \, , \cdots \, , L$. Note that $w^n_i, w^n_{i+1} \in \Omega \Rightarrow p_j(\bar{w}_{i+1/2}) > 0$ for $j = 1 \, , \cdots \, , L$, and $\lim\limits_{\gamma \to +\infty} \widetilde{w}^{L,*}_{i+1/2} = \lim\limits_{\gamma \to +\infty} \widetilde{w}^{R,*}_{i+1/2} = \bar{w}_{i+1/2}$. According to the continuity of the functions p_j, this implies the existence of a γ large enough such that $p_j(\widetilde{w}^{L,*}_{i+1/2}) > 0$ and $p_j(\widetilde{w}^{R,*}_{i+1/2}) > 0$ for all $j = 1, \cdots L$, which ensures the robustness property and is consistent with the previous Lemma. Of course, this limit value of γ may depend on the functions $(p_j)_{j=1,\cdots,L}$ involved in the definition of Ω. However, an explicit treshold can be exhibited under some additional regularity hypothesis. More precisely, let us assume that the functions p_j admit local Taylor expansions at order $N_j \in \mathbb{N}^*$ such that:

$$\left| p_j(x+h) - \left(p_j(x) + \sum_{k=1}^{N_j} \frac{1}{k!} dp^k_{j,x}(h) \right) \right| \leq \frac{M_j}{(N_j+1)!} \|h\|^{N_j+1} \quad , \quad \forall x, h \in \mathbb{R}^d \, ,$$

with $M_j > 0$ and where $dp^k_{j,x}(h)$ is the *k-th* order differential of p_j at point x. Note that, as will be illustrated later, all the models considered in this paper enter this frame.

In what follows we will drop the subscript "j" for simplification purposes. Also, when no confusion is possible, we will drop the subscript "$i + 1/2$" and rewrite (2.8), (2.9) as:

$$\widetilde{w}^* = \bar{w} + \nu \, \delta w \, , \tag{3.2}$$

where $\nu = \dfrac{\lambda}{\lambda+\gamma}$ and $(\widetilde{w}^*, \delta w)$ being either equal to $(\widetilde{w}^{L,*}_{i+1/2}, w^{L,*}_{i+1/2} - \bar{w}_{i+1/2})$ or $(\widetilde{w}^{R,*}_{i+1/2}, w^{R,*}_{i+1/2} - \bar{w}_{i+1/2})$. Then, according to (3.2), we have:

$$\left| p(\widetilde{w}^*) - \left(p(\bar{w}) + \sum_{k=1}^{N} \frac{1}{k!} \nu^k dp^k_{\bar{w}}(\delta w) \right) \right| \leq \frac{M}{(N+1)!} |\nu|^{N+1} \|\delta w\|^{N+1}, \tag{3.3}$$

from which we deduce a sufficient condition to have $p(\widetilde{w}^*) > 0$:

$$p(\bar{w}) + \sum_{k=1}^{N} \frac{1}{k!} \nu^k dp^k_{\bar{w}}(\delta w) - \frac{M}{(N+1)!} |\nu|^{N+1} \|\delta w\|^{N+1} > 0\,. \tag{3.4}$$

Recalling that $\lambda \geq 0$ and $\gamma \geq 0$, we set $\mu = \lambda + \gamma > 0$. Then, multiplying (3.4) by μ^{N+1}, we can express the previous condition through the positivity of a polynomial of order $N+1$ in μ:

$$Q(\mu) := \mu Q_1(\mu) - \frac{M}{(N+1)!} |\lambda|^{N+1} \|\delta w\|^{N+1} > 0\,, \tag{3.5}$$

where

$$Q_1(\mu) = \mu^N p(\bar{w}) + \sum_{k=1}^{N} \frac{1}{k!} \lambda^k \mu^{N-k} dp^k_{\bar{w}}(\delta w). \tag{3.6}$$

Note that the polynomial (3.5) only depends on $\bar{w}$ and δw, which are explicit interface quantities independent from γ, according to (3.2). From this, we remark that the dominant term of Q is $\mu^{N+1} p(\bar{w}) \geq 0$, so that the study of the roots of Q will allow to identify a real value μ^+ such that $Q(\mu) > 0$ for all $\mu > \mu^+$, or in an equivalent way, for all $\gamma \geq 0$ satisfying:

$$\gamma > \mu^+ - \lambda\,. \tag{3.7}$$

We have thus established the following result:

Lemma 3.2. *Assume that Ω is under the form (3.1), and consider $(w_i^n)_{i\in\mathbb{Z}}$ a given sequence in Ω. Let w_i^{n+1} be given by the viscous scheme (2.6). Let Δt be restricted according to the CFL-like condition (2.5). Then, if the viscous constant $\gamma \geq 0$ satisfies the condition:*

$$\gamma > \max_{i\in\mathbb{Z}} \left(\max_{j=1,\cdots,L} \left(\mu_j^+ - \lambda_{i+1/2} \right) \right),$$

where μ_j^+ is the largest root of the polynomial Q defined in (3.5), we have $w_i^{n+1} \in \Omega$ for all $i \in \mathbb{Z}$.

Remark 1. *Example of the Shallow Water equations :*
We have $\Omega = \left\{ w \in \mathbb{R}^d,\, p(w) > 0 \right\}$ with $p(w) = h$ and $d = 2, 3$. We have (3.3) with $N = 1$ and $M = 0$:

$$p(\widetilde{w}^*) = p(\bar{w}) + \nu \delta w.\nabla p = \bar{h} + \nu \delta h\,,$$

Since $M = 0$, the sufficient condition (3.5) reduces to $Q_1(\mu) > 0$, that is:

$$(\lambda + \gamma)\, \bar{h} + \lambda \delta h > 0\,,$$

from which we deduce the condition:

$$\gamma > -\lambda \frac{h^*}{\bar{h}}, \tag{3.8}$$

with $h^* = \delta h + \bar{h}$. *One may remark that if the original scheme is robust, i.e. the intermediate states* $h^{L,*}_{i+1/2}, h^{R,*}_{i+1/2}$ *given by (2.2), (2.3) are positive, then* $h^* > 0$ *and there is no condition on* γ.

REMARK 2. *Let us also remark that the case of isentropic gas dynamics, similar to what we previously said for shallow water, would not pose problems in the case of vacuum. Indeed, if a given intercell we have* $h_i \to 0^+, h_{i+1} > 0$, *then we get*

$$\tilde{h}^{L*}_{i+1/2} = \frac{h_i + h_{i+1}}{2} + \frac{\lambda}{\lambda + \gamma} \left(h^{L*}_{i+1/2} - \frac{h_i + h_{i+1}}{2} \right).$$

If $h^*_{i+1/2} - \frac{h_i + h_{i+1}}{2} \geq 0$, *then* $\tilde{h}^{L*}_{i+1/2} \geq 0$ *and no additional restrictions are required for* γ. *This would be for instance the case when the original scheme is robust.*
If $h^*_{i+1/2} - \frac{h_i + h_{i+1}}{2} < 0$, *then* $h^{L*}_{i+1/2} \geq 0$ *provided that* $\gamma \geq -\frac{2\lambda h^*_{i+1/2}}{h_i + h_{i+1}}$, *which should be enforced in order to have a robust scheme. Remark that the right hand side of the inequality for the second case corresponds to (3.8) and remains bounded for* $h_i \to 0^+$.

In the general case, for compressible Euler equations, the phase state

$$\Omega = \{(\rho, \rho u, \rho E) \text{ st. } \rho > 0 \text{ and } \rho E - (\rho u^2)/(2\rho) > 0\}$$

is not convex. Hence, the procedure described in this section does not apply for a numerical scheme expressed in the conservative variables $w = (\rho, \rho u, \rho E)$. *Moreover, the technique would be applied to the conserved variables, but here we would have an extra difficulty as the internal energy should remain positive as well. In practice, we have checked for the double rarefaction test case that the Roe scheme computes complex values of the speed of sound near vacuum (because of too small values of the total enthalpy in the approximated Riemann solver), which cannot be corrected by simply adding the* γ*-correction.*

4. Artificial viscosity and discrete entropy inequalities. In order to get the discrete entropy inequality (1.6), we apply for an entropy preserving sufficient condition established by Harten, Lax and van Leer in [48]. For the sake of completeness, we recall this result and the reader is referred to [48] for the proof.

LEMMA 4.1 (Harten, Lax and van Leer [48]). *Let* w^n_i *and* w^n_{i+1} *be given in* Ω. *Assume that the approximate Riemann solver satisfies*

$$\frac{1}{\Delta x} \int_{-\Delta x/2}^{\Delta x/2} \eta \left(\bar{\mathcal{W}}^{\mathcal{R}} \left(\frac{x}{\Delta t}; w^n_i, w^n_{i+1} \right) \right) dx \leq \frac{1}{2} \left(\eta(w^n_i) + \eta(w^n_{i+1}) \right) - \frac{\Delta t}{\Delta x} \left(G(w^n_{i+1}) - G(w^n_i) \right), \tag{4.1}$$

for a given entropy pair (η, G). *Then, the Godunov-type scheme (2.6) satisfies a discrete entropy inequality (1.6) where the numerical entropy flux function reads as*

follows:

$$G_\Delta(w_i^n, w_{i+1}^n) = G(w_{i+1}^n) - \frac{\Delta x}{2\Delta t}\eta(w_{i+1}^n) + \frac{1}{\Delta x}\int_0^{\Delta x/2} \eta\left(\bar{\mathcal{W}}^{\mathcal{R}}\left(\frac{x}{\Delta t}; w_i^n, w_{i+1}^n\right)\right)\, dx,$$
$$= G(w_{i+1}^n) + \lambda_{i+\frac{1}{2}}\eta(w_{i+\frac{1}{2}}^{R\star}) + (\lambda_{i+\frac{1}{2}} + \gamma)(\eta(\bar{w}_{i+\frac{1}{2}}) - \eta(w_{i+1}^n)).$$

Now, equipped with such a result, the expected discrete entropy inequality (1.6) is obtained as soon as the inequality (4.1) is proved to be satisfied. Since the approximate Riemann solver is given by (2.1), we easily get

$$\frac{1}{\Delta x}\int_{-\Delta x/2}^{\Delta x/2} \eta\left(\bar{\mathcal{W}}^{\mathcal{R}}\left(\frac{x}{\Delta t}; w_i^n, w_{i+1}^n\right)\right)\, dx = \left(\frac{1}{2} - (\lambda_{i+\frac{1}{2}} + \gamma)\frac{\Delta t}{\Delta x}\right)\left(\eta(w_i^n) + \eta(w_{i+1}^n)\right)$$
$$+ 2\gamma\frac{\Delta t}{\Delta x}\eta(\bar{w}_{i+\frac{1}{2}}) + \lambda_{i+\frac{1}{2}}\frac{\Delta t}{\Delta x}\left(\eta(w_{i+\frac{1}{2}}^{L\star}) + \eta(w_{i+\frac{1}{2}}^{R\star})\right),$$

so that the inequality (4.1) recasts as follows:

$$\mathcal{E}_{i+\frac{1}{2}}^0 + \gamma\mathcal{D}_{i+\frac{1}{2}} \leq 0, \tag{4.2}$$

where the quantities $\mathcal{E}_{i+\frac{1}{2}}^0$ and $\mathcal{D}_{i+\frac{1}{2}}$ are defined by (2.12) and (2.13). It is worth noticing that $\mathcal{E}_{i+\frac{1}{2}}^0$ is nothing but an entropy dissipation rate associated with the original scheme (1.4) while $\mathcal{E}_{i+\frac{1}{2}}^0 + \gamma\mathcal{D}_{i+\frac{1}{2}}$ stands for the entropy dissipation rate of the viscous scheme (1.7). Since η is a convex function, we immediately get $\mathcal{D}_{i+\frac{1}{2}} \leq 0$, which coincides with an entropy dissipation rate associated with the artificial viscosity.

Now, we remark that $\mathcal{E}_{i+\frac{1}{2}}^0$ is non-positive for an entropy preserving scheme (1.4). Then, the expected inequality (4.1) is immediately satisfied. But, as soon as the original scheme (1.4) is entropy violating, we have $\mathcal{E}_{i+\frac{1}{2}}^0 > 0$. However, we notice that neither $\mathcal{E}_{i+\frac{1}{2}}^0$ nor $\mathcal{D}_{i+\frac{1}{2}}$ depends on γ. As a consequence, the objective now is to fix $\gamma \geq 0$ large enough such that the required inequality (4.2) holds true. In fact, a particular attention must be paid on a possible blow-up of γ. Indeed, after (2.14), γ may eventually go to infinity as $\mathcal{D}_{i+\frac{1}{2}}$ goes to zero. In the next statement, we establish that γ remains bounded.

LEMMA 4.2. *Let $(w_i^n)_{i\in\mathbb{Z}}$ be given in Ω. Let w_i^{n+1} be given by the viscous scheme (2.6), or equivalently (1.7). Assume that the discretization of the non-conservation product $A(w)\partial_x w$ satisfies (2.11). Assume $\lambda_{i+\frac{1}{2}} > \lambda^\star$. Let Δt be restricted according to the CFL-like restriction (2.5). Moreover, let the Hessian matrix $\nabla_w^2\eta(w)$ be positive definite. Then, $\gamma \geq 0$, given by (2.14), is bounded and the discrete entropy inequality (1.6) is satisfied.*

Proof. After Lemma 4.1, the expected discrete entropy inequality (1.6) holds as soon as (4.2) is verified. As a consequence, the proof is completed when the quantity $-\mathcal{E}_{i+\frac{1}{2}}^0/\mathcal{D}_{i+\frac{1}{2}}$ is proved to be bounded for $\mathcal{E}_{i+\frac{1}{2}}^0 \geq 0$. Since η is a convex function with $\nabla_w^2\eta(w)$ a positive definite matrix, $\mathcal{D}_{i+\frac{1}{2}} = 0$ if and only if $w_i^n = w_{i+1}^n$. We now study the behavior of $-\mathcal{E}_{i+\frac{1}{2}}^0/\mathcal{D}_{i+\frac{1}{2}}$ near $w_i^n = w_{i+1}^n$. To address such an issue, let us first introduce

$$w_{i+\frac{1}{2}}^{HLL} = \frac{1}{2\lambda_{i+\frac{1}{2}}\Delta t^2}\int_0^{\Delta t}\int_{-\lambda_{i+\frac{1}{2}}\Delta t}^{\lambda_{i+\frac{1}{2}}\Delta t} \mathcal{W}_{ex}\left(\frac{x}{\Delta t}; w_i^n, w_{i+1}^n\right)\, dx\, dt. \tag{4.3}$$

In fact, this specific sate, introduced in [48], plays an essential role in the derivation of discrete entropy inequalities. Since $\mathcal{W}_{ex}\left(\frac{x}{\Delta t};w_i^n,w_{i+1}^n\right)$ is solution of (1.1), it satisfies

$$\partial_t \mathcal{W}_{ex} + \partial_x f(\mathcal{W}_{ex}) + A(\mathcal{W}_{ex})\partial_x \mathcal{W}_{ex} = 0.$$

The integration of the above relation over $(-\lambda_{i+\frac{1}{2}}\Delta t, \lambda_{i+\frac{1}{2}}\Delta t)\times(0,\Delta t)$, with $\lambda_{i+\frac{1}{2}}$ large enough and according (1.2), gives

$$\begin{aligned}\frac{1}{2\lambda_{i+\frac{1}{2}}\Delta t^2}\int_0^{\Delta t}\int_{-\lambda_{i+\frac{1}{2}}\Delta t}^{\lambda_{i+\frac{1}{2}}\Delta t}\mathcal{W}_{ex}\left(\frac{x}{\Delta t};w_i^n,w_{i+1}^n\right)\,dx\,dt = \\ \frac{1}{2}(w_i^n+w_{i+1}^n)-\frac{1}{2\lambda_{i+\frac{1}{2}}}\left(f(w_{i+1}^n)-f(w_{i+1}^n)\right) \\ -\frac{1}{2\lambda_{i+\frac{1}{2}}\Delta t}\int_0^{\Delta t}\int_{-\lambda_{i+\frac{1}{2}}\Delta t}^{\lambda_{i+\frac{1}{2}}\Delta t}A\left(\mathcal{W}_{ex}\left(\frac{x}{t};w_i^n,w_{i+1}^n\right)\right)\partial_x\mathcal{W}_{ex}\left(\frac{x}{t};w_i^n,w_{i+1}^n\right)\,dx\,dt.\end{aligned}$$

Arguing (2.11), we obtain

$$\begin{aligned}w_{i+\frac{1}{2}}^{HLL} = \frac{1}{2}(w_i^n+w_{i+1}^n)-\frac{1}{2\lambda_{i+\frac{1}{2}}}\left(f(w_{i+1}^n)-f(w_{i+1}^n)\right) \\ -\frac{1}{4\lambda_{i+\frac{1}{2}}}\left(A_\Delta^L(w_i^n,w_{i+1}^n)+A_\Delta^R(w_i^n,w_{i+1}^n)\right)\cdot(w_{i+1}^n-w_i^n).\end{aligned}$$

Now, let us notice that

$$w_{i+\frac{1}{2}}^{HLL} = \frac{1}{2}\left(w_{i+\frac{1}{2}}^{L\star}+w_{i+\frac{1}{2}}^{R\star}\right), \tag{4.4}$$

where $w_{i+\frac{1}{2}}^{L,R\star}$ are given by (2.2) and (2.3).

Moreover, since $\mathcal{W}_{ex}$, is defined as an exact solution of (1.1), necessarily it satisfies the entropy inequality (1.3) so that we have

$$\partial_t\eta(\mathcal{W}_{ex})+\partial_x G(\mathcal{W}_{ex})\le 0.$$

Once again, integrating the above inequality over $(-\lambda_{i+\frac{1}{2}}\Delta t, \lambda_{i+\frac{1}{2}}\Delta t)\times(0,\Delta t)$, because of (1.2), we get

$$\begin{aligned}\frac{1}{2\lambda_{i+\frac{1}{2}}\Delta t}\int_{-\lambda_{i+\frac{1}{2}}\Delta t}^{\lambda_{i+\frac{1}{2}}\Delta t}\eta\left(\mathcal{W}_{ex}\left(\frac{x}{t};w_i^n,w_{i+1}^n\right)\right)\,dx \le \\ \frac{1}{2}\left(\eta(w_i^n)+\eta(w_{i+1}^n)\right)-\frac{1}{2\lambda_{i+\frac{1}{2}}}\left(G(w_{i+1}^n)-G(w_i^n)\right).\end{aligned}$$

Arguing the well-known Jensen's inequality, from (4.3) the above inequality reads

$$\eta(w_{i+\frac{1}{2}}^{HLL})\le\frac{1}{2}(w_i^n+w_{i+1}^n)-\frac{1}{2\lambda_{i+\frac{1}{2}}}\left(G(w_{i+1}^n)-G(w_i^n)\right).$$

Next, with $\mathcal{E}_{i+\frac{1}{2}}^0$ defined by (2.12), we obtain the following estimation:

$$\mathcal{E}_{i+\frac{1}{2}}^0\le\lambda_{i+\frac{1}{2}}\left(\eta(w_{i+\frac{1}{2}}^{L\star})+\eta(w_{i+\frac{1}{2}}^{R\star})-2\eta(w_{i+\frac{1}{2}}^{HLL})\right),$$

to write according to (2.13)

$$0 \leq -\frac{\mathcal{E}^0_{i+\frac{1}{2}}}{\mathcal{D}_{i+\frac{1}{2}}} \leq \lambda_{i+\frac{1}{2}} \frac{\eta(w^{L\star}_{i+\frac{1}{2}}) - \eta(w^{R\star}_{i+\frac{1}{2}}) - 2\eta\left(\frac{1}{2}(w^{L\star}_{i+\frac{1}{2}} + w^{R\star}_{i+\frac{1}{2}})\right)}{\eta(w^n_i) - \eta(w^n_{i+1}) - 2\eta\left(\frac{1}{2}(w^n_i + w^n_{i+1})\right).} \tag{4.5}$$

Now, arguing the definition of $w^{L\star}_{i+\frac{1}{2}}$ and $w^{R\star}_{i+\frac{1}{2}}$, given by (2.2) and (2.3), an usual asymptotic expansion in the neighbourhood of $w^n_i = w^n_{i+1}$ easily gives

$$\frac{\eta(w^{L\star}_{i+\frac{1}{2}}) - \eta(w^{R\star}_{i+\frac{1}{2}}) - 2\eta\left(\frac{1}{2}(w^{L\star}_{i+\frac{1}{2}} + w^{R\star}_{i+\frac{1}{2}})\right)}{\eta(w^n_i) - \eta(w^n_{i+1}) - 2\eta\left(\frac{1}{2}(w^n_i + w^n_{i+1})\right).} = \mathcal{O}(1),$$

and the proof is achieved. □

5. Numerical experiments. In this section we present several examples to illustrate the efficiency of the proposed stability enforcing technique. First, we perform numerical approximations of the solutions of the isentropic gas dynamic model. We show the ability of the here designed technique to stabilize entropy violating schemes. Next, we present an application of the proposed technique to the numerical approximation of the one layer shallow-water system with flat bathymetry to correct the VF-Roe scheme and, finally, an application to the bi-layer shallow-water model.

5.1. Compressible Euler equations. We consider the 1-D evolution of a compressible inviscid fluid of density ρ, velocity u, pressure p and specific total energy E and we denote by $e = E - \frac{1}{2}u^2$ the specific internal energy. This evolution is governed by the 1-D Euler equations which read:

$$\begin{cases} \partial_t \rho + \partial_x(\rho u) = 0, \\ \partial_t(\rho u) + \partial_x(\rho u^2 + p(\rho, e)) = 0, \\ \partial_t(\rho E) + \partial_x(\rho E u + p(\rho, e)u) = 0. \end{cases} \tag{5.1}$$

The pressure function is given by an ideal gas equation of state: $p(\rho, e) = (\Gamma - 1)\rho e$ where the heat capacity ratio is $\Gamma = 1.4$. Denoting $w = (\rho, \rho u, \rho E)^T$ and $f(w) = (\rho u, \rho u^2 + p(\rho, e), \rho E u + p(\rho, e)u)^T$ system (5.1) can be written:

$$\partial_t w + \partial_x f(w) = 0. \tag{5.2}$$

This system admits a family of entropy/entropy flux functions given by

$$\eta(w) = \rho\varphi(p/\rho^\Gamma), \quad G(w) = \eta(w)u,$$

where φ is a smooth function which satisfies the restrictions derived in [48] (see also in [72]). In the following, we will consider the entropies $\eta_i(w) = \rho\varphi_i(p/\rho^\Gamma)$ given by the following three functions:

$$\varphi_1(\theta) = \ln(\theta), \quad \varphi_2(\theta) = -\theta^{1/(\Gamma+1)}, \quad \varphi_3(\theta) = \theta^{-\frac{2}{\Gamma}}.$$

The adopted initial scheme (1.6) is given by the VF-Roe method [38] which is known to be entropy violating for some test-cases. The corrected scheme (1.7) is obtained by defining the numerical viscosity parameter γ ensuring a discrete entropy inequality for the entropy $\eta_1(w) = \rho\varphi_1(p/\rho^\Gamma)$. Consequently, an interesting issue is to know whether the entropy inequality for the other two entropies is satisfied or not.

5.1.1. A smooth solution. We consider the smooth initial data given by:

$$u_0(x) = 1, \quad p_0(x) = 1, \quad \rho_0(x) = \begin{cases} 1 + \exp\Big(-\frac{1}{1-x^2}\Big), & |x| \leq 1, \\ 1, & |x| \geq 1. \end{cases}$$

for which the exact solution is smooth and given by: $u(x,t) = 1$, $p(x,t) = 1$, $\rho(x,t) = \rho_0(x-t)$. The computations have been run on the time interval $[0, 0.5]$ with grids given by the following space steps : $\Delta x = 2/N$ with $N = 100 \times 2^j$ with $j \in \{0, .., 5\}$. For this smooth solution, the VF-Roe scheme is entropy satisfying. Hence the corrected scheme rigorously coincide with the original scheme, the artificial viscosity γ is always zero and the discrete entropy (in)equalities are satisfied for all the entropies $\eta_i(w)$ for $i = 1, 2, 3$. Figure 5.1 displays the density at the final time and the numerical convergence of the L^1-norm of the error between the numerical solution and the exact solution. We observe a first order (with respect to Δx) convergence which is what is expected for this smooth solution.

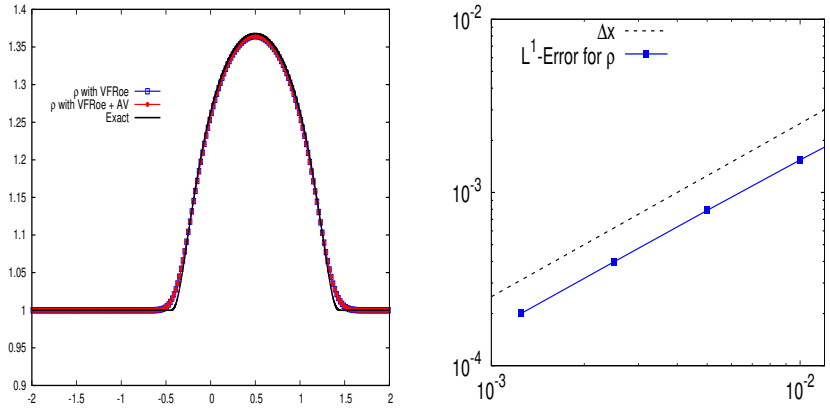

Fig. 5.1: Left: space variations of the density at the final time $t = 0.5$. Mesh size: 100 cells. Right: L^1-error with respect to Δx.

5.1.2. A Riemann problem. We consider the Riemann problem given by the following initial data:

$$\rho_0(x) = \begin{cases} 1.0, & x < 0, \\ 0.25, & x > 0. \end{cases} \quad u_0(x) = 0.0, \quad p_0(x) = \begin{cases} 1.0, & x < 0, \\ 0.1, & x > 0. \end{cases}$$

The computations have been run on the time interval $[0, 0.2]$ with grids given by the following space steps : $\Delta x = 1/N$ with $N = 100 \times 2^j$ with $j \in \{0, .., 5\}$. For this Riemann-type solution, the VF-Roe scheme is still expected to be entropy satisfying. In practice, we observe that, for all mesh sizes, the artificial viscosity is activated only in the first two time steps near the initial discontinuity. On the first time step, the maximum value of γ is $\gamma_{\max} = 1.53$ and the ratio $\gamma/\lambda_{i+\frac{1}{2}}$ satisfies $(\gamma/\lambda_{i+\frac{1}{2}})_{\max} = 0.75$. On the second time step, we have respectively $\gamma_{\max} = 0.48$ and $(\gamma/\lambda_{i+\frac{1}{2}})_{\max} = 0.26$, and these values do not depend on the mesh size. For all the following time steps, we observe that $\gamma = 0$ and that the VF-Roe scheme is entropy satisfying not only for η_1 but also for η_2 and η_3. Figure 5.2 displays the density, velocity and pressure at

the final time and the numerical convergence of the L^1-norm of the error for these variables. We observe a convergence with an order slightly larger than 0.5 (with respect to Δx) which is the expected order of convergence for this solution with a contact discontinuity.

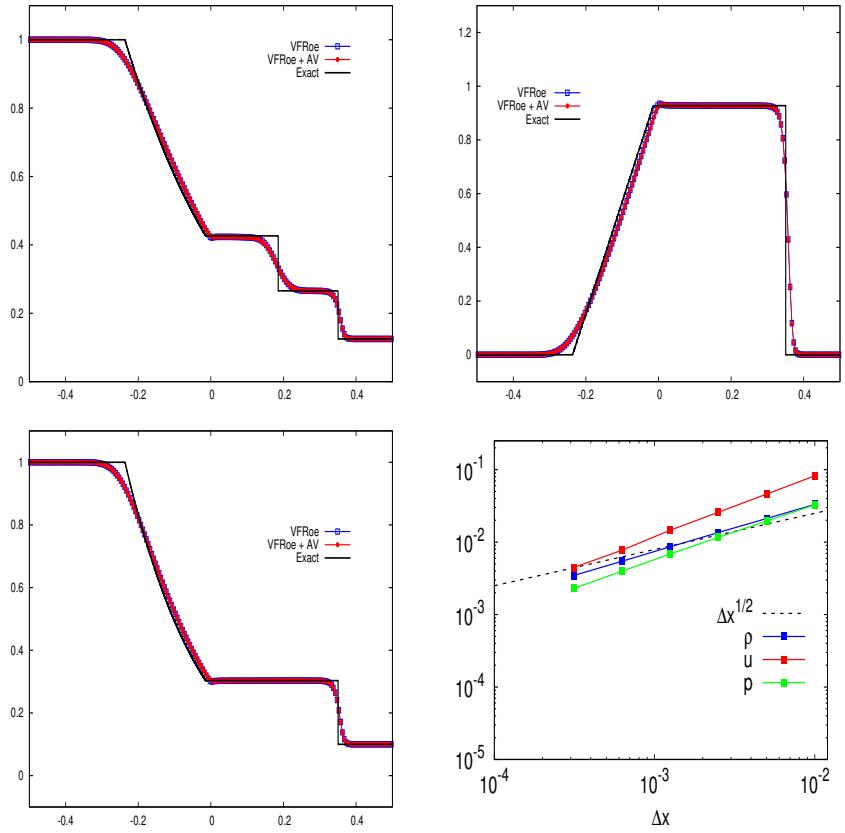

Fig. 5.2: Space variations at the final time $t = 0.2$ of the density (upper-left), velocity (upper-right) and pressure (lower-left). Mesh size: 100 cells. Lower-right: L^1-error with respect to Δx.

5.1.3. A Riemann problem with a sonic rarefaction wave. We consider the Riemann problem given by the following initial data:

$$\rho_0(x) = \begin{cases} 1.0, & x < 0, \\ 0.25, & x > 0. \end{cases} \qquad u_0(x) = 0.0, \qquad p_0(x) = \begin{cases} 1.0, & x < 0, \\ 0.01, & x > 0. \end{cases}$$

The computations have been run on the time interval $[0, 0.25]$ with grids given by the following space steps : $\Delta x = 1/N$ with $N = 100 \times 2^j$ with $j \in \{0, .., 10\}$. For this Riemann-type solution, the VF-Roe scheme is known to produce a steady non entropic discontinuity at the sonic point of the rarefaction wave. This discontinuity generates a production of (mathematical) entropy at the discrete level which can be balanced thanks to the artificial viscosity term in the corrected scheme.

Figure 5.3 displays the density, velocity and pressure at the final time for the VFRoe scheme with and without correction and for a Suliciu relaxation scheme (which is very similar to the HLLC scheme and is known to be entropy-satisfying, referred to as *Relax* in the figure). We also display the numerical convergence of the L^1-norm of the error for these variables, for the VFRoe scheme with and without correction . We observe that without the artificial viscosity correction, the VF-Roe scheme does not converge because of the steady non-entropic discontinuity at $x = 0$. When the scheme is corrected with the artificial viscosity, the amplitude of the non entropic discontinuity gets smaller as the mesh is refined enabling the approximate solution to converge towards the exact solution with an order slightly larger than 0.5. For a fixed mesh however, the relaxation scheme performs slightly better than the corrected VFRoe scheme since it displays no artificial discontinuity in the rarefaction wave.

Contrary to the previous test-case (with no sonic point in the rarefaction wave), we observe here that the artificial viscosity correction is regularly activated during the whole computation. However, the maximum values of γ and $\gamma/\lambda_{i+\frac{1}{2}}$ are obtained at the second time step with $\gamma_{\max} = 0.6$ and $(\gamma/\lambda_{i+\frac{1}{2}})_{\max} = 0.28$ and these maximum values do not depend on the mesh size. It is to be noted that the algorithmic complexity of the corrected scheme is comparable to that of the entropy-satisfying relaxation scheme. Indeed, for 800 cells, the computation lasts $6s$ with the relaxation scheme, while it lasts $7s$ with the corrected VFRoe scheme.

By construction, the numerical method is entropy-satisfying for η_1. However, one can check that the approximate solution also satisfies discrete entropy inequalities for η_2 and η_3. In Table 5.1 we present the value of the L^1-norm of the positive part of the entropy budget, defined as the left hand side of inequality (1.6), obtained with both the original VF-Roe scheme and with the corrected scheme. We can see that, even for η_2 and η_3, while the VF-Roe scheme produces entropy, the corrected scheme preserves a local discrete entropy inequality.

Mesh size	η_1		η_2		η_3	
100	1.05e-06	$<$ e-14	4.40e-07	$<$ e-14	1.49e-06	$<$ e-14
400	3.29e-07	$<$ e-14	1.37e-07	$<$ e-14	4.69e-07	$<$ e-14
1600	3.43e-08	$<$ e-14	1.43e-08	$<$ e-14	4.901e-08	$<$ e-14
6400	4.33e-09	$<$ e-14	1.80e-09	$<$ e-14	6.20e-09	$<$ e-14
25600	1.53e-09	$<$ e-14	6.38e-10	$<$ e-14	2.19e-09	$<$ e-14
102400	1.24e-09	$<$ e-14	5.14e-10	$<$ e-14	1.77e-09	$<$ e-14

Table 5.1: L^1-norm of the positive part of the entropy budget for the three mathematical entropies η_1, η_2, η_3. Left columns: VF-Roe scheme. Right columns: VF-Roe scheme with artificial viscosity.

5.2. Shallow-water equations. We now consider the well-known shallow water equations on a flat bottom:

$$\begin{cases} \partial_t h + \partial_x q = 0, \\ \partial_t q + \partial_x \left(\dfrac{q^2}{h} + \dfrac{1}{2} g h^2 \right) = 0 \,, \end{cases} \tag{5.3}$$

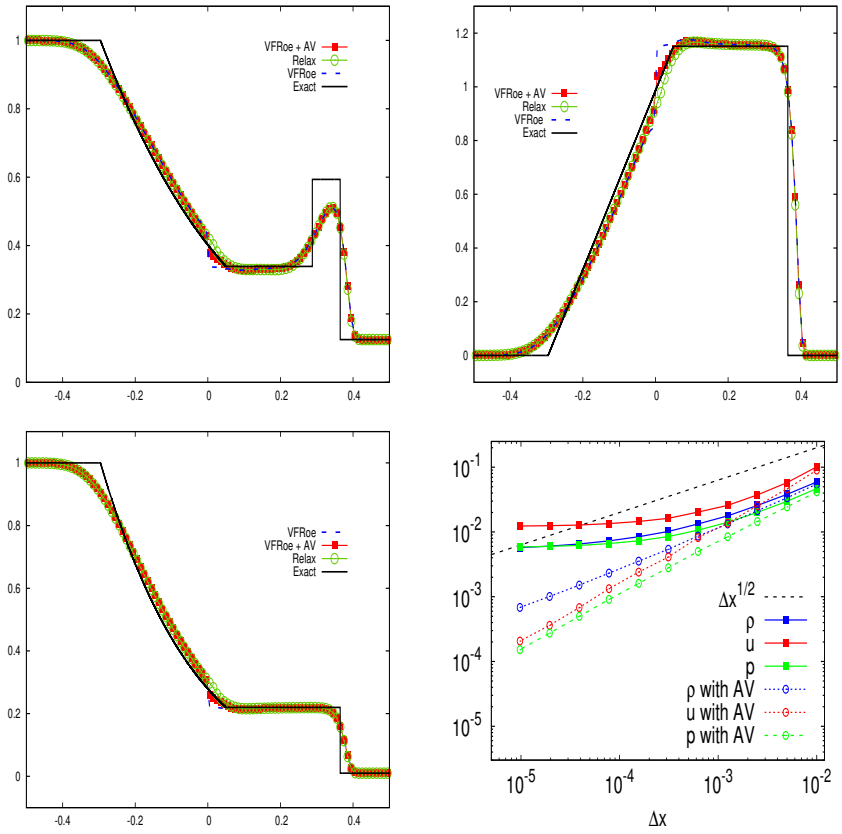

Fig. 5.3: Space variations at the final time $t = 0.2$ of the density (upper-left), velocity (upper-right) and pressure (lower-left). Mesh size: 100 cells. Lower-right: L^1-error with respect to Δx. In the legend, *Relax* refers to the Suliciu relaxation scheme.

where $h = h(x,t)$ and $q = q(x,t)$ refer to the water height and discharge respectively. Gathering the flow variables in the vector $w = (h,q)^T$ and setting $f(w) = (q, q^2/h + gh^2/2)^T$, the system can be written on the form (5.2). We recall that the mechanical energy $\eta(w) = \dfrac{1}{2}hu^2 + \dfrac{1}{2}gh^2$ plays the role of a mathematical entropy associated to the entropy flux $G(w) = \left(\eta(w) + \dfrac{1}{2}gh^2\right)u$.

5.2.1. Dam-break problems. As previously, we consider the entropy-violating VF-Roe scheme to exhibit the regularizing virtues of the proposed methodology. We first consider the following dam-break problem:

$$h(x,0) = \begin{cases} 1.5, & x < 12.5, \\ 0.02, & x > 12.5, \end{cases} \qquad u(x,0) = 0.0\,,$$

on the computational domain $[0,25]$ with $\Delta x = 0.0025\,m$, with a final time $T = 0.1\,s$. As in Test-case 5.1.3, this initial condition leads to an entropy-violating discontinuity at the level of the rarefaction wave.

This phenomenon can be observed in Figure 5.4, which displays the water height and velocity profiles associated with the original VF-Roe scheme and the corrected version of the scheme, together with the energy budget, computed on the basis of (1.6). We observe that without correction the VF-Roe scheme produces an entropy-violating solution characterized by a sudden growth of entropy at the sonic point $x = 12.5m$. As expected, the artificial viscosity is able to correct this failure.

Concerning convergence analysis, depicted in Figure 5.4 (*bottom right*), computations have been run on a series of regular meshes with space step $\Delta x = 1/N$ with $N = 100 \times 2^j$ with $j \in \{0, .., 8\}$. We clearly see that the VF-Roe scheme does not converge and that the introduction of artificial viscosity allows to recover a proper convergence for both flow variables.

The time evolution of the ratio $(\gamma/\lambda_{i+\frac{1}{2}})_{\max}$ is proposed in Figure 5.5 for $\Delta x = 0.0025\, m$. It can be observed that it is especially during the first iterations that artificial viscosity must be introduced to ensure entropy stability, while a small correction is still required throughout the simulation. Nevertheless, the maximum value of this ratio is around 6.935e-02 and induces a minor increase of the computational time, according to the time step restriction (2.5). Note that this time behavior do not depend on the space resolution, which is in accordance with the previous test-cases.

Next, we propose to analyze more specifically the robustness property of the scheme, in particular the condition (2.15), which resumes to (3.8) in the case of Shallow Water equations. To this purpose we consider now the same left initial state but impose $h(x) = 0$ if $x > 12.5$. Computations are run on a mesh of 1000 elements, with a purely centered scheme. The numerical stability comes therefore only from the viscous terms carried by the constant γ issuing from conditions (2.14), (2.15), which time evolution is given in Figure 5.6. Note that the robustness condition (2.15) is regularly dominant in this case and thus mainly controls the calibration of the numerical viscosity. Here again, the resulting value of γ is relatively low compared to the maximum wave speed λ. We can observe on Figure 5.6 the velocity and water height profiles at final time $T = 0.8s$, which show that we are able to recover a quite stable simulation in spite of a non-positive and entropy-violating basis scheme.
Nevertheless, we would like to mention here that the procedure to guarantee the robustness should be used with caution. In some case indeed it can lead to very large (but still bounded) values of gamma, making the strategy unworkable. This problem appears to be dependant of the choice of model parameters and remains sensitive to the cutoff strategies used to discriminate dry cells. The goal here is to illustrate that artificial viscosity can indeed be used to guarantee the robustness of the schemes, but further analytical work needs to be done to ensure a robust systematic procedure.

5.2.2. Double rarefaction wave in the presence of vacuum. We now show that the proposed method is compatible with occurrence of dry states. To that purpose we use the test case employed in [76] consisting of a Riemann problem which solution is composed of two rarefaction waves, with a dry zone occurring between the two waves. This test case stands for a relevant benchmark to highlight the difficulty for solvers to deal with vacuum (see for instance [61]), and [17] [39] for an adaptation of this test to non trivial topography. Considering the computational domain $[-10, 10]$, the initial condition is the following:

$$h(x,0) = 10\,, \quad u(x,0) = \begin{cases} -35, & x < 0, \\ 35, & x > 0. \end{cases}$$

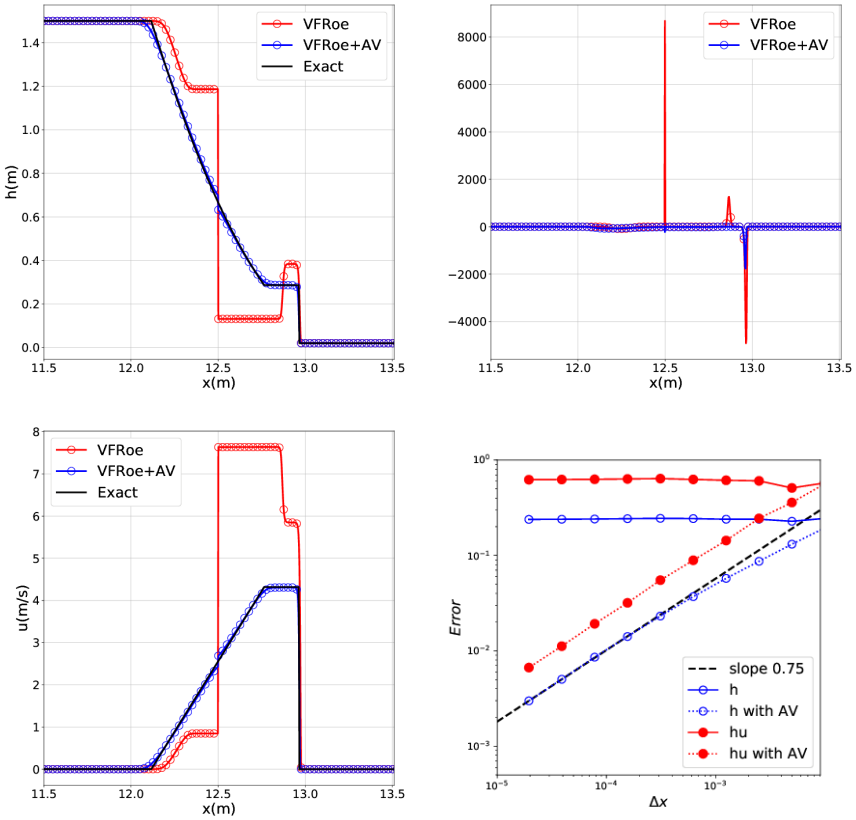

Fig. 5.4: Space variations at the final time $T = 0.1s$ of the water height (upper-left), energy budget (upper-right) and velocity (lower-left). Mesh size: 10 000 cells. Lower-right: L^1-error with respect to Δx.

Neumann boundary conditions are imposed at the boundaries. Numerical results obtained with the Roe solver supplemented by artificial viscosity are given in Figure 5.8 at final time $T = 0.125s$.

We observe a proper propagation of the rarefaction waves, implying a water height close to zero at the center of the domain as expected. Based on the space distribution of the local ratio γ/λ, we note that a subsequent amount of viscosity is needed to ensure stability, notably at the reconnection points with the initial constant states. It should be mentioned also that the minimum value of h during the simulation is about 1.e-04, which is not sufficiently small to threaten the stability of the scheme: the positivity condition (2.15) is not activated for this test. Note that without correction the scheme is unstable and did not provide any exploitable result. Similar observations were made with the VFRoe and HLL schemes.

5.3. Bi-layer shallow-water system. We consider the homogeneous bi-layer 1-D shallow water system (see [21]):

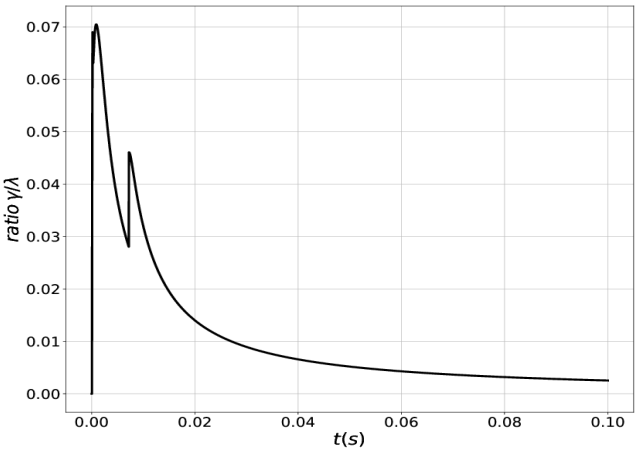

Fig. 5.5: Time evolution of the maximum ratio γ/λ.

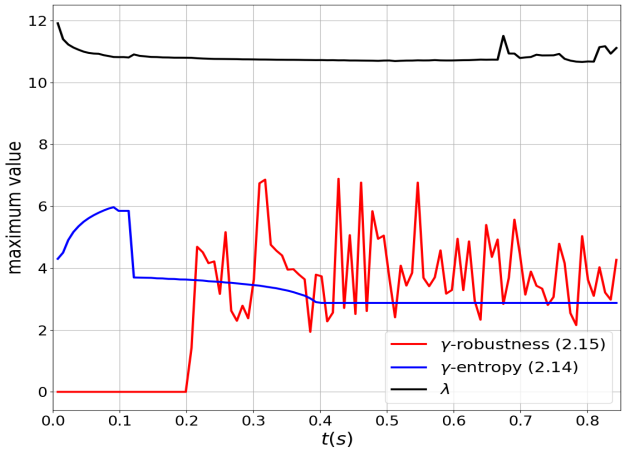

Fig. 5.6: Time evolution of the quantities λ and γ given by the conditions (2.14) and (2.15) for the dam break problem with dry front.

$$\begin{cases} \partial_t h_1 + \partial_x q_1 = 0, \\ \partial_t q_1 + \partial_x \left(\dfrac{q_1^2}{h_1} + \dfrac{1}{2} g h_1^2 \right) = -g h_1 \partial_x h_2, \\ \partial_t h_2 + \partial_x q_2 = 0, \\ \partial_t q_2 + \partial_x \left(\dfrac{q_2^2}{h_2} + \dfrac{1}{2} g h_2^2 \right) = -\dfrac{\rho_1}{\rho_2} g h_2 \partial_x h_1. \end{cases} \tag{5.4}$$

Index 1 refers to the upper layer while index 2 refers to the lower layer. This

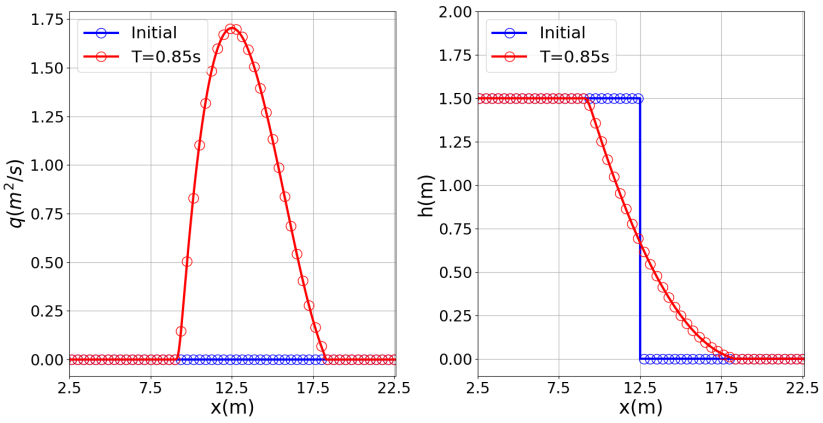

Fig. 5.7: Velocity and water height profiles at time $T = 0.8s$ for the dam break problem with dry front.

system uses the following notation:

- $h_j = h_j(x,t) \geq 0$ is the thickness of the j-th layer at the section of coordinate x at time t.
- $q_j = q_j(x,t)$ is the discharge of the j-th layer at the section of coordinate x at time t and is related with the averaged velocity at each layer by the following relation: $q_j = u_j h_j$, $j = 1,\ 2$.
- g is the gravitational constant.
- ρ_j refers to the constant density of the j-th layer with $\rho_1 < \rho_2$.

The bottom is assumed to be flat. This system can be written in the form

$$\partial_t w + \partial_x f(w) + A(w)\partial_x w = 0, \tag{5.5}$$

where

$$w = \begin{pmatrix} h_1 \\ q_1 \\ h_2 \\ q_2 \end{pmatrix}, \quad f(w) = \begin{pmatrix} q_1 \\ \dfrac{q_1^2}{h_1} + \dfrac{1}{2}gh_1^2 \\ q_2 \\ \dfrac{q_2^2}{h_2} + \dfrac{1}{2}gh_2^2 \end{pmatrix},$$

$$A(w) = \begin{pmatrix} 0 & 0 & 0 & 0 \\ 0 & 0 & gh_1 & 0 \\ 0 & 0 & 0 & 0 \\ grh_2 & 0 & 0 & 0 \end{pmatrix},$$

with $r = \rho_1/\rho_2$.

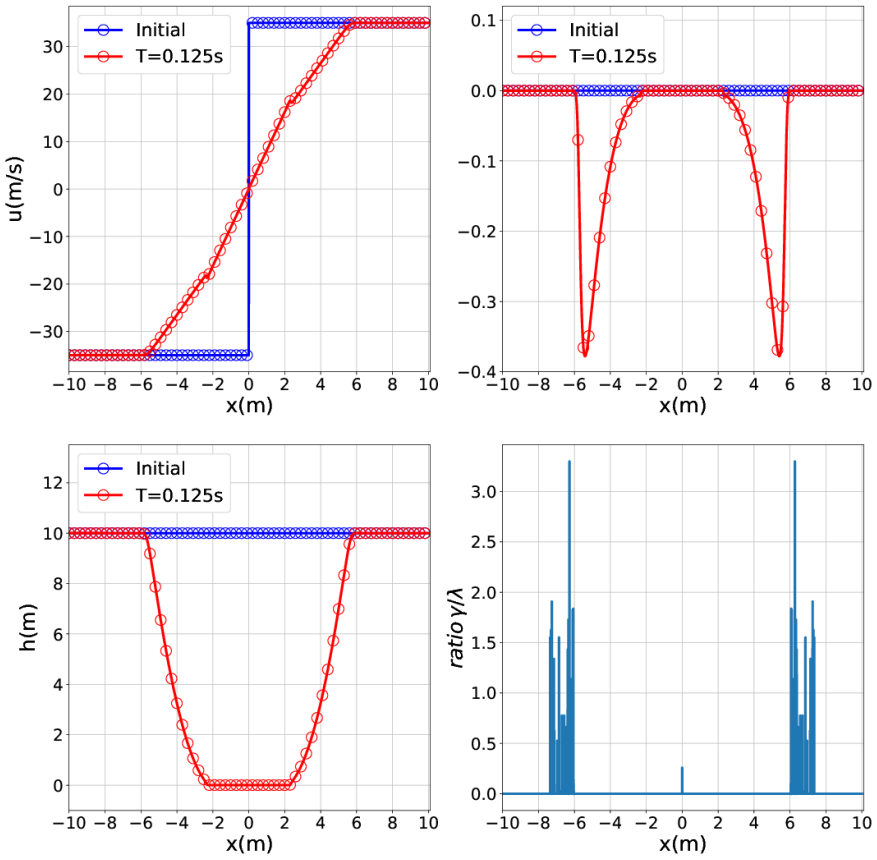

Fig. 5.8: Space variations at the final time $T = 0.125s$ of the velocity height (upper-left), energy budget (upper-right) and water height (lower-left), together with the ratio γ/λ (lower-right) Mesh size: 10 000 cells.

An entropy-entropy flux pair for the bi-layer shallow water system is given by

$$\eta(w) = \sum_{j=1}^{2} \rho_j \left(h_j \frac{u_j^2}{2} + g \frac{h_j^2}{2} \right) + g\rho_1 h_1 h_2 \tag{5.6a}$$

$$G(w) = \sum_{j=1}^{2} \rho_j \left(h_j \frac{u_j^2}{2} + g h_j^2 \right) u_j + \rho_1 g h_1 h_2 (u_1 + u_2). \tag{5.6b}$$

The wave speeds are the eigenvalues of $\mathcal{A}(w) = J(w) + A(w) = \nabla_w f(w) + A(w)$, that is, the roots of the characteristic polynomial:

$$p(\lambda) = (\lambda^2 - 2u_1\lambda + u_1^2 - gh_1)(\lambda^2 - 2u_2\lambda + u_2^2 - gh_2) - rgh_1gh_2. \tag{5.7}$$

When $r \cong 1$, first order approximations of the eigenvalues were given in [69]:

$$\lambda_{ext}^{\pm} = \frac{u_1 h_1 + u_2 h_2}{h_1 + h_2} \pm \sqrt{g(h_1 + h_2)}, \tag{5.8}$$

$$\lambda_{int}^{\pm} = \frac{u_1 h_2 + u_2 h_1}{h_1 + h_2} \pm \sqrt{g' \frac{h_1 h_2}{h_1 + h_2} \left(1 - \frac{(u_1 - u_2)^2}{g'(h_1 + h_2)}\right)}, \tag{5.9}$$

where $g' = (1 - r)g$.

The exact expression of the eigenvalues can be obtained by using Ferrari's method to find an analytical solution for quartic equations. For each eigenvalue λ, an associated eigenvector is given by:

$$R_i = \begin{pmatrix} 1 \\ \lambda \\ \mu \\ \lambda\mu \end{pmatrix}, \tag{5.10}$$

where:

$$\mu = \frac{(\lambda - u_1)^2}{g h_1} - 1.$$

An important difficulty of system (5.4) is related to the loss of hyperbolicity: for $r \cong 1$ this situation occurs approximately when the following inequality is satisfied:

$$\mathcal{F}_r^2 = \frac{(u_1 - u_2)^2}{g'(h_1 + h_2)} > 1. \tag{5.11}$$

This loss of hyperbolicity is related to the appearance of shear instabilities that may lead, in real flows, to intense mixing of the two layers. While, in practice, this mixture partially dissipates the energy, in numerical experiments these interface disturbances may grow and overwhelm the solution. Obviously, a simple model based on two layer of immiscible fluids is not able to simulate the mixing processes due to the development of shear instabilities: a more complex multilayer model or a continuously stratified model would be required. In [28] authors propose a simple strategy consisting on adding an extra friction term in order to get rid of the related instabilities and go beyond of them by reaching again the hyperbolic character.

Here, we consider a standard path-conservative Roe solver for system (5.5) based on the family of straight segments

$$\Phi(s; w_L, w_R) = w_L + s(w_R - w_L)$$

described in [21]. The numerical scheme reads as follows:

$$\begin{aligned} w_i^{n+1} = w_i^n &- \frac{\Delta t}{\Delta x} \left(f_\Delta(w_i^n, w_{i+1}^n) - f_\Delta(w_{i-1}^n, w_i^n) \right) \\ &- \frac{\Delta t}{2\Delta x} \left(A_\Delta^L(w_i^n, w_{i+1}^n) \cdot (w_{i+1}^n - w_i^n) + A_\Delta^R(w_{i-1}^n, w_i^n) \cdot (w_i^n - w_{i-1}^n) \right), \end{aligned} \tag{5.12}$$

where the numerical flux is given by

$$f_\Delta(w_i^n, w_{i+1}^n) = \frac{1}{2}\left(f(w_i^n) + f(w_{i+1}^n)\right) - \frac{1}{2}|\mathcal{A}_\Delta^n| \cdot (w_{i+1}^n - w_i^n), \tag{5.13}$$

where $\mathcal{A}_\Delta^n$ is a Roe matrix according to the choice of segment-path and is defined as follows

$$\mathcal{A}_\Delta = \begin{pmatrix} 0 & 1 & 0 & 0 \\ gh_{\Delta,1} - u_{\Delta,1}^2 & 2u_{\Delta,1} & gh_{\Delta,2} & 0 \\ 0 & 0 & 0 & 1 \\ rgh_{\Delta,1} & 0 & gh_{\Delta,2} - u_{\Delta,2}^2 & 2u_{\Delta,2} \end{pmatrix}, \tag{5.14}$$

where we have dropped the time dependency for simplicity. In (5.14), $h_{\Delta,j}$ and $u_{\Delta,j}$, $j = 1,\ 2$ are the Roe averages and are defined as

$$h_{\Delta,j} = \frac{h_{i,j} + h_{i+1,j}}{2}, \quad u_{\Delta,j} = \frac{\sqrt{h_{i,j}}u_{i,j} + \sqrt{h_{i+1,j}}u_{i+1,j}}{\sqrt{h_{i,j}} + \sqrt{h_{i+1,j}}}, \quad j = 1,\ 2.$$

As usual, $|\mathcal{A}_\Delta^n|$ is the matrix that has the same eigenvectors than matrix $\mathcal{A}_\Delta^n$ and whose eigenvalues are the absolute value of those of $\mathcal{A}_\Delta^n$. Finally,

$$A_\Delta^L(w_i^n, w_{i+1}^n) = A_\Delta^R(w_i^n, w_{i+1}^n) = \begin{pmatrix} 0 & 0 & 0 & 0 \\ 0 & 0 & gh_{\Delta,1} & 0 \\ 0 & 0 & 0 & 0 \\ grh_{\Delta,2} & 0 & 0 & 0 \end{pmatrix}. \tag{5.15}$$

When $\mathcal{A}_\Delta$ has complex eigenvalues, this matrix is no more a Roe linearization in the usual sense. Nevertheless, the numerical scheme (5.12)-(5.15) can still be applied by redefining $\mathcal{A}_\Delta$. Following [28], we consider the real Jordan decomposition of $\mathcal{A}_\Delta$, that is,

$$\mathcal{A}_\Delta = \mathcal{K}_\Delta \cdot \mathcal{L}_\Delta \cdot \mathcal{K}_\Delta^{-1},$$

where $\mathcal{L}_\Delta$ is a block diagonal matrix whose diagonal blocks are either the real eigenvalues or 2×2 blocks of the form:

$$\begin{bmatrix} \alpha & \beta \\ -\beta & \alpha \end{bmatrix} \tag{5.16}$$

associated to every pair of conjugate complex eigenvalues $\alpha \pm \mathrm{i}\beta$. $\mathcal{K}_\Delta$ is the real matrix corresponding to the change of basis. Now, $|\mathcal{A}_\Delta|$ can be formally defined by setting $|\mathcal{L}_\Delta|$ as the diagonal matrix obtained from the Jordan matrix by taking the absolute values of the real eigenvalues and by replacing the diagonal blocks (5.16) corresponding to a pair of conjugate complex eigenvalues by the diagonal block:

$$\begin{bmatrix} \sqrt{\alpha^2 + \beta^2} & 0 \\ 0 & \sqrt{\alpha^2 + \beta^2} \end{bmatrix}.$$

5.3.1. Riemann problem. Let us consider the following Riemann problem:

$$h_1(x,0) = \begin{cases} 0.95 & \text{if } x < 0 \\ 0.05 & \text{otherwise,} \end{cases} \qquad h_2(x,0) = 1 - h_1(x,0), \quad u_1(x,0) = u_2(x,0) = 0,$$

in the interval $[-1,1]$ with $\Delta x = 0.005$ and $CFL = 0.4$. Open boundary conditions are set and $r = 0.2$. We approximate the solution of this Riemann problem with the usual Roe scheme and with Roe scheme with the artificial viscosity method described in this paper.

Figure 5.9 shows the free surface and interface computed with both schemes at times $t = 1$ and 2 s. At it can be observed, a non-entropic shock is created by Roe scheme at $x = 0$, while it disappears when the artificial viscosity scheme is used. Similar behaviour is observed when plotting the velocities (see Figure 5.10).

As we have done previously, we show the time evolution of the ratio $(\gamma/\lambda_{i+\frac{1}{2}})_{\max}$ in Figure 5.11 for $\Delta x = 0.005\,m$. Again, one can observe that it is during the first iterations that artificial viscosity must be introduced to ensure entropic stability, while a small correction is still required throughout the simulation. The maximum value of this ratio is around 0.0315.

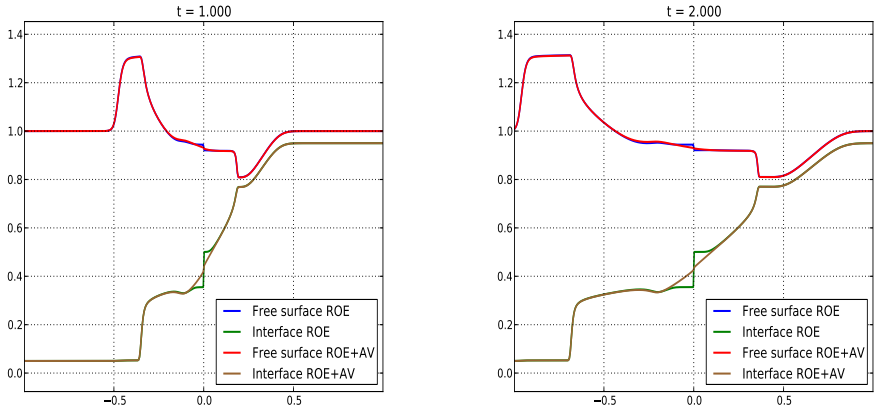

(a) $t = 1\,s$ (b) $t = 2\,s$

Fig. 5.9: Test 1: Free surface and interface: comparison between Roe scheme (blue and green lines) and Roe with artificial viscosity (red and brown lines).

5.3.2. Non-hyperbolic regime. This test was inspired by Test 1 introduced in [28]. It consists on the evolution of a perturbation of shear two-layer fluid that is close to the unstable region (appearance of complex eigenvalues). The simulation is carried out on a flat channel described by the interval $[-5,5]$. The initial condition is given by

$$h_1(x,0) = 0.4 - 0.1e^{-16x^2}, \quad h_2(x,0) = 1.0 - h_1(x,0),$$

$$u_1(x,0) = 0.15, \quad u_2(x,0) = -0.15.$$

Free boundary conditions are imposed and the system is simulated during $T = 10$ s. The CFL parameter is set to 0.4 and $\Delta x = 0.01$ and $r = 0.99$. Note that

$$\mathcal{F}_r^2 = \frac{(u_1 - u_2)^2}{g'(h_1 + h_2)} \approx 0.917$$

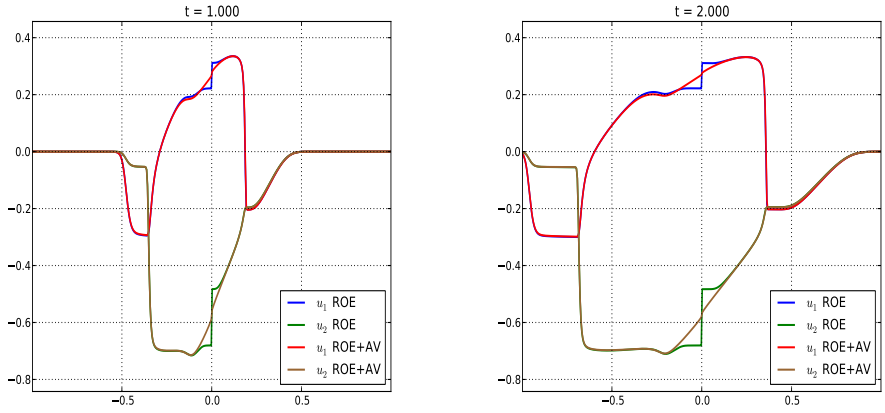

(a) $t = 1\,s$ (b) $t = 2\,s$

Fig. 5.10: Test 1: Velocities at each layers: comparison between Roe scheme (blue and green lines) and Roe with artificial viscosity (red and brown lines).

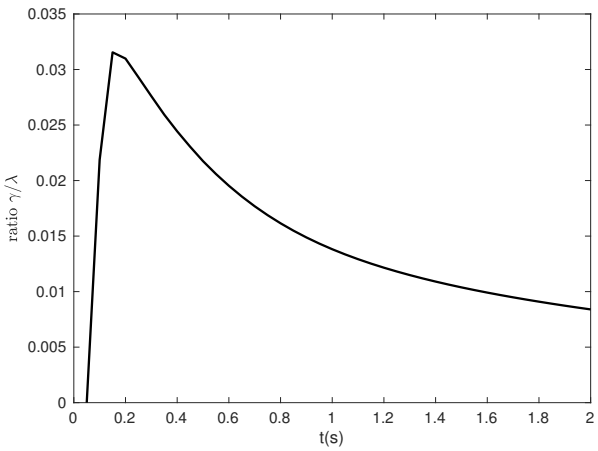

Fig. 5.11: Time evolution of the maximum ratio γ/λ.

at every point at time $t = 0\,s$. Recall that values of $\mathcal{F}_r^2$ close to 1 result in the appearance of complex eigenvalues. Due to the perturbation on the interface, the bi-layer system becomes unstable near the region where the perturbation is located. On the one hand, these instabilities propagate along the channel if the previous Roe solver is used and the numerical scheme drives towards a completely useless result. On the other hand, adding properly some artificial viscosity to control the entropy of the system, allows to perform a stable simulation. Of course, it is impossible to properly simulate such complex fluid with a simple bi-layer shallow water system, but the artificial viscosity allows to provide some stable simulation that could be seen as

the best approximation that could be obtained with the bi-layer shallow-water system.

Figure 5.12 shows the free surface and the interface evolution at $t = 5$ and $10\,s$ obtained with Roe scheme previously described (left) and with the Roe scheme with the artificial viscosity technique to control the entropy (right). As expected, the initial perturbation grows in time when Roe scheme is applied, producing non-physical waves, while the Roe scheme combined with the artificial viscosity technique is able to produce stable simulations. Similar results can be observed for the velocities (see Figure 5.13). Figure 5.14 shows the evolution of the stability number $\mathcal{F}_r^2$ (5.11) at the same time steps. It is clear that the strong oscillations obtained with the Roe scheme are nonphysical, while the solution obtained with the Roe scheme with artificial viscosity is the best approximation that one could obtain with the bi-layer shallow-water system for such complex shear flows. In this case, the time evolution of the ratio $(\gamma/\lambda_{i+\frac{1}{2}})_{\max}$ in Figure 5.15 shows large values and it is present in the whole simulation, although the maximum values occur during the initial iterations.

5.3.3. Comparison with unstable scheme. Let us now consider the Riemann problem given by

$$h_1(x,0) = \begin{cases} 0.8 & \text{if } x < 0 \\ 0.2 & \text{otherwise,} \end{cases} \qquad h_2(x,0) = 1 - h_1(x,0), \quad u_1(x,0) = u_2(x,0) = 0,$$

in the interval $[-5, 5]$ with $\Delta x = 0.002$ and $CFL = 0.5$. Open boundary conditions are set and $r = 0.99$. We consider the unconditional unstable central scheme (without any numerical viscosity) and its correction with the artificial viscosity method described in this paper.

As expected the central scheme blows up at finite time ($t = 0.1005841$ in this test). Nevertheless, the artificial viscosity method is able to stabilize the scheme, providing a good solution. Figure 5.16 show the comparison at time $t = 0.05$, before the blow up. Figure 5.17 shows the final time $t = 5.0$ where the solution is compared with a Roe scheme.

Acknowledgements. Manuel J. Castro acknowledges financial support from the Spanish Government and FEDER through the coordinated Research project RTI2018-096064-B-C21 and the Andalusian Government Research projects UMA18-FEDERJA-161 and P18-RT-3163. Arnaud Duran acknowledges financial support from the French National Research Agency project NABUCO, grant ANR-17-CE40-0025 and from the French National program INSU-CNRS (Institut National des Sciences de l´Univers - Centre National de la Recherche Scientifique) program LEFE-MANU (Les Enveloppes Fluides et Environnement - Méthodes Mathématiques et Numériques), project DWAVE. Tomás Morales acknowledges financial support from the Spanish Government and FEDER through the coordinated Research project RTI2018-096064-B-C22.

Data availability statement. The datasets generated during and/or analysed during the current study are available from the corresponding author on reasonable request.

Declarations. The authors have no relevant financial or non-financial interests to disclose

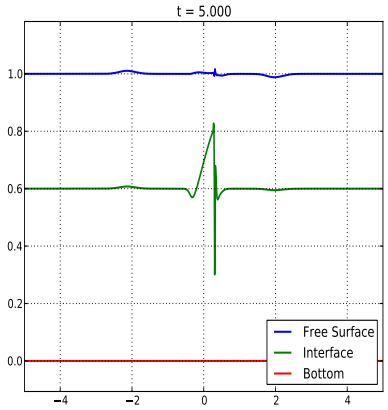

(a) $t = 5\,s$

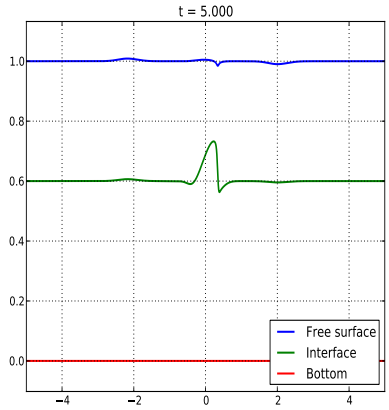

(b) $t = 5\,s$

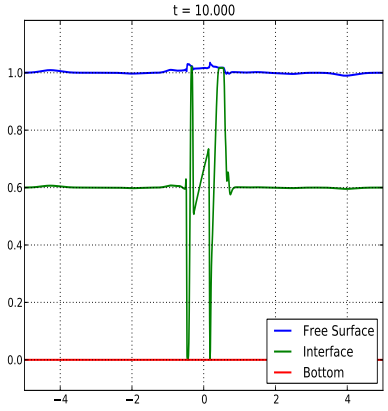

(c) $t = 10.0\,s$

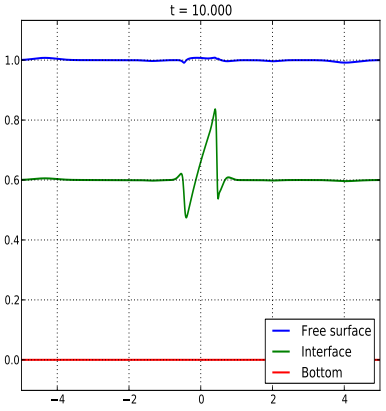

(d) $t = 10.0\,s$

Fig. 5.12: Test 2: Free surface and interface evolution. Roe scheme (left column). Roe scheme with artificial viscosity (right column).

[1] R. Abgrall. A general framework to construct schemes satisfying additional conservation relations. application to entropy conservative and entropy dissipative schemes. *Journal of Computational Physics*, 372:640–666, 2018.

[2] R. Abgrall, P. Bacigaluppi, and S. Tokareva. A high-order nonconservative approach for hyperbolic equations in fluid dynamics. *Computers & Fluids*, 169:10–22, jun 2018.

[3] R. Abgrall, S. Busto, and M. Dumbser. A simple and general framework for the construction of thermodynamically compatible schemes for computational fluid and solid mechanics. *Applied Mathematics and Computation*, 440:127629, 2023.

[4] R. Abgrall and K. Ivanova. Staggered residual distribution scheme for compressible flow. *arXiv preprint arXiv:2111.10647*, 2021.

[5] R. Abgrall and S. Karni. A comment on the computation of non-conservative products. *Journal of Computational Physics*, 229(8):2759–2763, 2010.

[6] R. Abgrall, P. Öffner, and H. Ranocha. Reinterpretation and extension of entropy correction terms for residual distribution and discontinuous galerkin schemes: application to structure

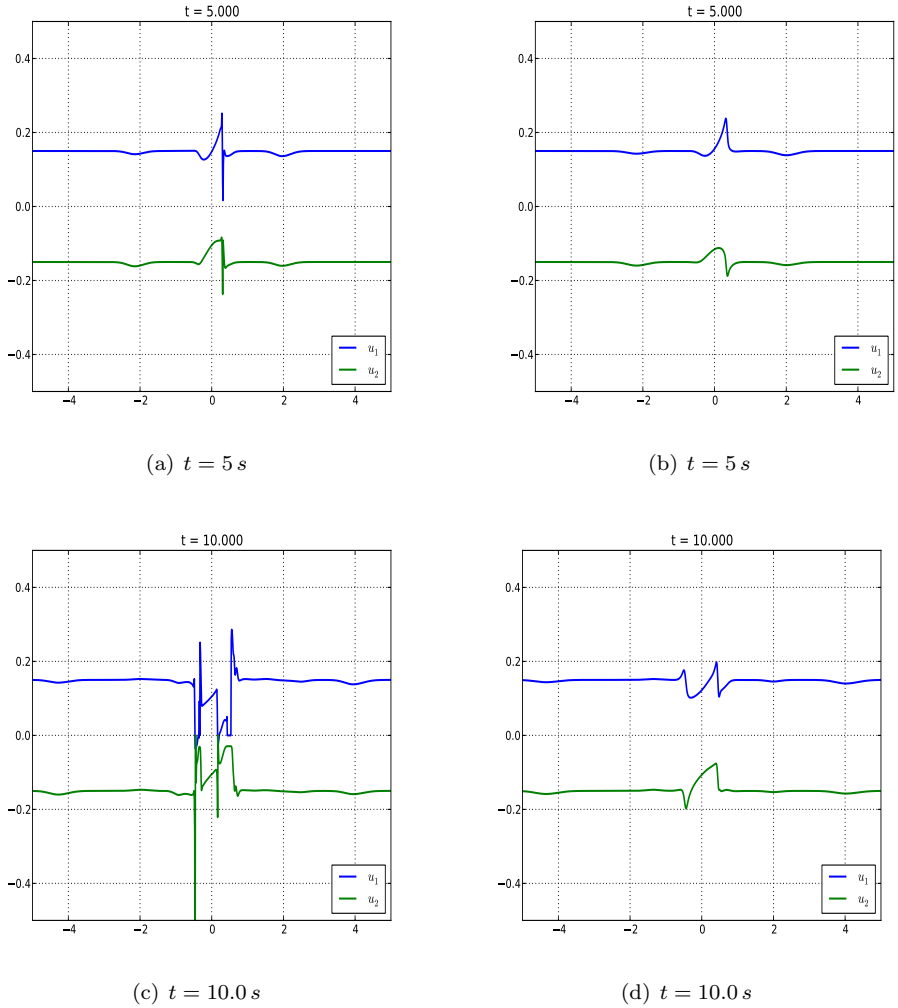

(a) $t = 5\,s$ (b) $t = 5\,s$

(c) $t = 10.0\,s$ (d) $t = 10.0\,s$

Fig. 5.13: Test 2: Velocities of the two layers. Roe scheme (left column). Roe scheme with artificial viscosity (right column).

preserving discretization. *Journal of Computational Physics*, 453:110955, 2022.

[7] Remi Abgrall and Harish Kumar. Numerical Approximation of a Compressible Multiphase System. *Communications in Computational Physics*, 15(5):1237–1265, May 2014.

[8] A. Beljadid, P. G. LeFloch, S. Mishra, and C. Parés. Schemes with well-controlled dissipation. hyperbolic systems in nonconservative form. *Communications in Computational Physics*, to appear, 2016.

[9] C. Berthon, B. Boutin, and R. Turpault. Shock profiles for the shallow-water Exner models. *Advances in Applied Mathematics and Mechanics*, 7(3):267–294, 2015.

[10] C. Berthon, F. Coquel, and P. G. LeFloch. Why many theories of shock waves are necessary: kinetic relations for non-conservative systems. *Proc. Roy. Soc. Edinburgh Sect. A*, 142(1):1–37, 2012.

[11] C. Berthon, B. Dubroca, and A. Sangam. A local entropy minimum principle for deriving entropy preserving schemes. *SIAM Journal on Numerical Analysis*, 50(2):468–491, 2012.

[12] C. Berthon, A. Duran, F. Foucher, K. Saleh, and J. de D. Zabsonré. Improvement of the

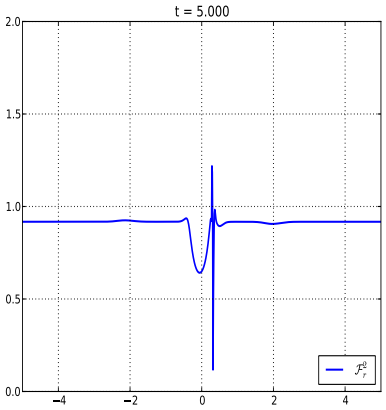

(a) $t = 5\,s$

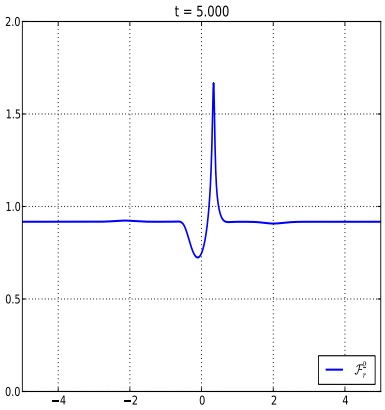

(b) $t = 5\,s$

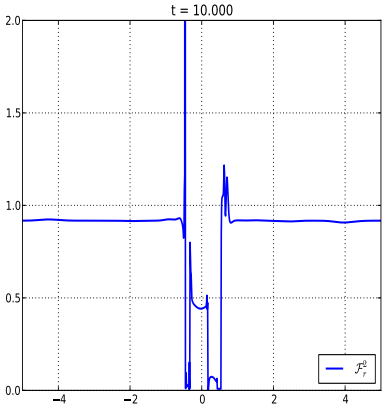

(c) $t = 10.0\,s$

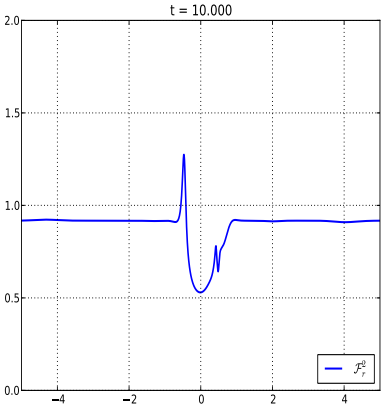

(d) $t = 10.0\,s$

Fig. 5.14: Test 2: Stability number $\mathcal{F}_r$. Roe scheme (left column). Roe scheme with artificial viscosity (right column).

hydrostatic reconstruction scheme to get fully discrete entropy inequalities. *Journal of Scientific Computing*, 80:924–956, 2019.

[13] C. Berthon, A. Duran, and K. Saleh. *Continuum Mechanics, Applied Mathematics and Scientific Computing : Godunov's Legacy*, chapter An easy control of the artificial numerical viscosity to get discrete entropy inequalities when approximating hyperbolic systems of conservation laws. Springer Nature Switzerland AG, 2020.

[14] Christophe Berthon and Frédéric Coquel. Nonlinear Projection Methods for Multi-Entropies Navier-Stokes Systems. *Mathematics of Computation*, 76(259):1163–1194, 2007.

[15] F. Bouchut. Introduction to the mathematical theory of kinetic equations. 1998.

[16] F. Bouchut. Entropy satisfying flux vector splittings and kinetic bgk models. *Numerische Mathematik*, 94(4):623–672, 2003.

[17] F. Bouchut. *Nonlinear stability of finite volume methods for hyperbolic conservation laws and well-balanced schemes for sources.* Frontiers in Mathematics. Birkhäuser Verlag, Basel, 2004.

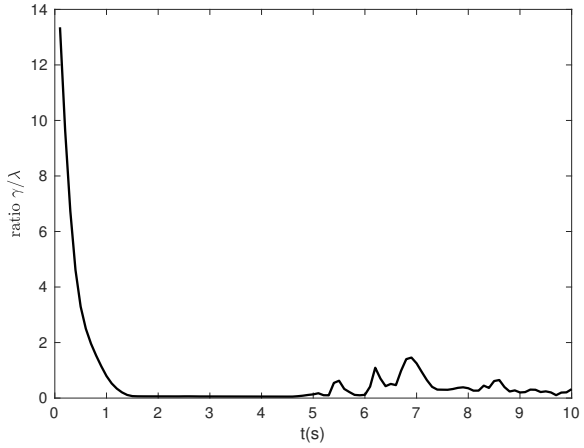

Fig. 5.15: Time evolution of the maximum ratio γ/λ.

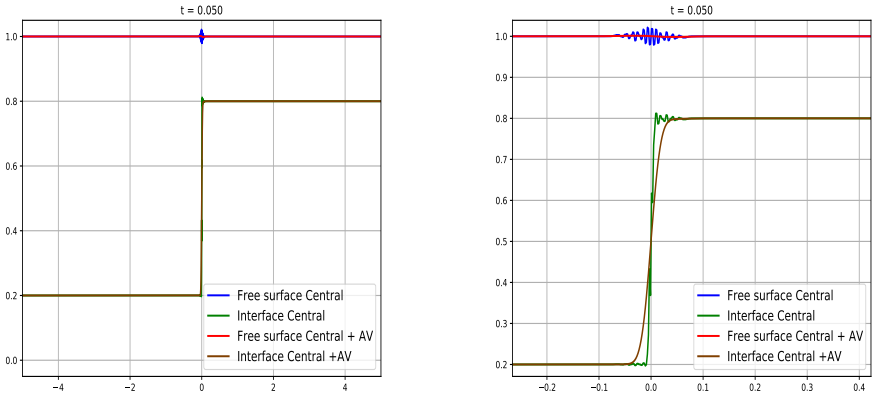

(a) $t = 1\,s$ (b) $t = 2\,s$

Fig. 5.16: Test 3: Free surface and interface: comparison between Central scheme (blue and green lines) and Central scheme with artificial viscosity (red and brown lines).

[18] F. Bouchut and T. Morales. A subsonic-well-balanced reconstruction scheme for shallow water flows. *SIAM Journal on Numerical Analysis*, 48(5):1733–1758, 2010.

[19] F. Bouchut and T. Morales de Luna. An entropy satisfying scheme for two-layer shallow water equations with uncoupled treatment. *M2AN Math. Model. Numer. Anal.*, 42(4):683–698, 2008.

[20] M. Castro, J. T. Frings, S. Noelle, C. Parés, and G. Puppo. On the hyperbolicity of two- and three-layer shallow water equations. In *Hyperbolic problems, theory, numerics and applications. Volume 1*, volume 17 of *Ser. Contemp. Appl. Math. CAM*, pages 337–345. World Sci. Publishing, Singapore, 2012.

[21] M. Castro, J. Macías, and C. Parés. A Q-scheme for a class of systems of coupled conservation

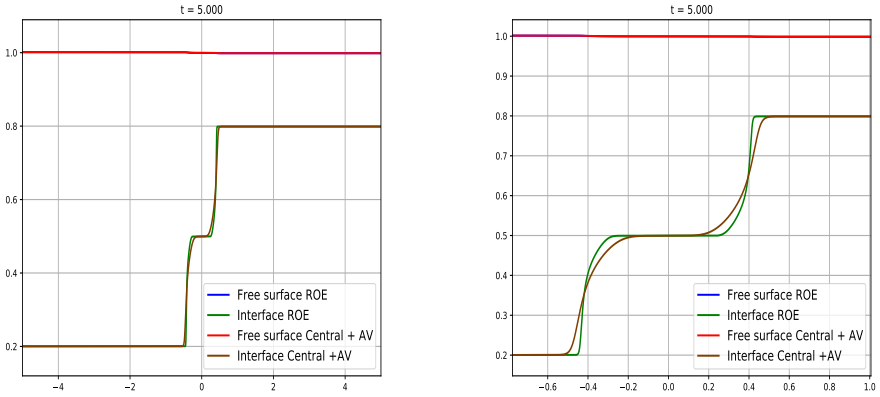

(a) $t = 1\,s$ (b) $t = 2\,s$

Fig. 5.17: Test 3: Free surface and interface: comparison between Roe scheme (blue and green lines) and Central scheme with artificial viscosity (red and brown lines).

laws with source term. Application to a two-layer 1-D shallow water system. *ESAIM: Mathematical Modelling and Numerical Analysis*, 35(01):107–127, 2001.

[22] M. J. Castro, P. G. LeFloch, M. L. Muñoz-Ruiz, and C. Parés. Why many theories of shock waves are necessary: convergence error in formally path-consistent schemes. *J. Comput. Phys.*, 227(17):8107–8129, 2008.

[23] M. J. Castro, J. Macías, C. Parés, J. A. García-Rodríguez, and E. Vázquez-Cendón. A two-layer finite volume model for flows through channels with irregular geometry: Computation of maximal exchange solutions: Application to the strait of gibraltar. *Communications in Nonlinear Science and Numerical Simulation*, 9(2):241–249, April 2004.

[24] M. J. Castro, T. Morales de Luna, and C. Parés. Well-Balanced Schemes and Path-Conservative Numerical Methods. In Rémi Abgrall and Chi-Wang Shu, editor, *Handbook of Numerical Analysis*, volume 18 of *Handbook of Numerical Methods for Hyperbolic ProblemsApplied and Modern Issues*, pages 131–175. Elsevier, 2017. DOI: 10.1016/bs.hna.2016.10.002.

[25] M.J. Castro, U. S. Fjordholm, S. Mishra, and C. Pares. Entropy conservative and entropy stable schemes for nonconservative hyperbolic systems. *SIAM Journal on Numerical Analysis*, 51(3):1371–1391, 2013.

[26] M. Castro Dıaz, E. D. Fernández-Nieto, T. Morales de Luna, G. Narbona-Reina, and C. Parés. A HLLC scheme for nonconservative hyperbolic problems. application to turbidity currents with sediment transport. *ESAIM: Mathematical Modelling and Numerical Analysis*, 47:1–32, 2013.

[27] M. J. Castro Díaz, T. Chacón Rebollo, E. D. Fernández-Nieto, and C. Parés. On well-balanced finite volume methods for nonconservative nonhomogeneous hyperbolic systems. *SIAM Journal on Scientific Computing*, 29(3):1093–1126, 2007.

[28] M. J. Castro-Díaz, E. D. Fernández-Nieto, J. M. González-Vida, and C. Parés-Madroñal. Numerical treatment of the loss of hyperbolicity of the two-layer shallow-water system. *Journal of Scientific Computing*, 48(1-3):16–40, 2011.

[29] C. Chalons and F. Coquel. The riemann problem for the multi-pressure euler system. *Journal of Hyperbolic Differential Equations*, 2(03):745–782, 2005.

[30] C. Chalons, F. Coquel, E. Godlewski, P.-A. Raviart, and N. Seguin. Godunov-type schemes for hyperbolic systems with parameter-dependent source. The case of Euler system with friction. *Math. Models Methods Appl. Sci.*, 20(11):2109–2166, 2010.

[31] Christophe Chalons. Path-conservative in-cell discontinuous reconstruction schemes for non conservative hyperbolic systems. *Communications in Mathematical Sciences*, 18(1):1–30, 2020.

[32] Alexandre Joel Chorin. Random choice solution of hyperbolic systems. *Journal of Computa-*

tional Physics, 22(4):517–533, dec 1976.

[33] F. Coquel and B. Perthame. Relaxation of energy and approximate Riemann solvers for general pressure laws in fluid dynamics. *SIAM Journal on Numerical Analysis*, 35(6):2223–2249, 1998.

[34] S. Cordier, M. H. Le, and T. Morales de Luna. Bedload transport in shallow water models: Why splitting (may) fail, how hyperbolicity (can) help. *Advances in Water Resources*, 34(8):980–989, 2011.

[35] C. M. Dafermos. *Hyperbolic conservation laws in continuum physics*, volume 325 of *Grundlehren der Mathematischen Wissenschaften [Fundamental Principles of Mathematical Sciences]*. Springer-Verlag, Berlin, third edition, 2010.

[36] G. Dal Maso, P. G. LeFloch, and F. Murat. Definition and weak stability of nonconservative products. *Journal de mathématiques pures et appliquées*, 74(6):483–548, 1995.

[37] F. Dubois and G Mehlman. A non-parameterized entropy correction for roe's approximate riemann solver. *Numer. Math.*, 73(73):169–208, 1996.

[38] T. Gallouët, J.-M. Hérard, and N. Seguin. Some recent finite volume schemes to compute Euler equations using real gas EOS. *International journal for numerical methods in fluids*, 39(12):1073–1138, 2002.

[39] T. Gallouët, J.-M. Hérard, and N. Seguin. Some approximate Godunov schemes to compute shallow-water equations with topography. *Computers & Fluids*, 32(4):479–513, 2003.

[40] J Glimm, E Isaacson, D Marchesin, and O McBryan. Front tracking for hyperbolic systems. *Advances in Applied Mathematics*, 2(1):91–119, mar 1981.

[41] J Glimm, D Marchesin, and O McBryan. A numerical method for two phase flow with an unstable interface. *Journal of Computational Physics*, 39(1):179–200, jan 1981.

[42] James Glimm. Solutions in the large for nonlinear hyperbolic systems of equations. *Communications on Pure and Applied Mathematics*, 18(4):697–715, nov 1965.

[43] E. Godlewski and P.-A. Raviart. *Hyperbolic systems of conservation laws*, volume 3/4 of *Mathématiques & Applications (Paris) [Mathematics and Applications]*. Ellipses, Paris, 1991.

[44] E. Godlewski and P.-A. Raviart. *Numerical approximation of hyperbolic systems of conservation laws*, volume 118 of *Applied Mathematical Sciences*. Springer-Verlag, New York, 1996.

[45] K. Godunov, G. A difference method for numerical calculation of discontinuous solutions of the equations of hydrodynamics. *Mat. Sb. (N.S.)*, 47(89):271–306, 1959.

[46] J.C. González-Aguirre, M.J. Castro, and T. Morales de Luna. A robust model for rapidly varying flows over movable bottom with suspended and bedload transport: Modelling and numerical approach. *Advances in Water Resources*, 140:103575, jun 2020.

[47] L. Gosse. *Computing Qualitatively Correct Approximations of Balance Laws: Exponential-fit, Well-balanced and Asymptotic-preserving*. Springer, 2013.

[48] Amiram Harten. On the symmetric form of systems of conservation laws with entropy. *Journal of Computational Physics*, 49(1):151–164, 1983.

[49] P. Helluy, J.-M. Hérard, H. Mathis, and S. Müller. A simple parameter-free entropy correction for approximate Riemann solvers. *Comptes rendus Mécanique*, 338(9):493–498, 2010.

[50] T. Y. Hou and P. G. LeFloch. Why nonconservative schemes converge to wrong solutions: error analysis. *Mathematics of computation*, 62(206):497–530, 1994.

[51] S. Karni. Viscous Shock Profiles and Primitive Formulations. *SIAM Journal on Numerical Analysis*, 29(6):1592–1609, 1992.

[52] B. Khobalatte and B. Perthame. Maximum principle on the entropy and second-order kinetic schemes. *Math. Comp.*, 62(205):119–131, 1994.

[53] D. Kröner. *Numerical schemes for conservation laws*. Wiley-Teubner Series Advances in Numerical Mathematics. John Wiley & Sons Ltd., Chichester, 1997.

[54] P.D. Lax. Shock waves and entropy. In *Contributions to nonlinear functional analysis (Proc. Sympos., Math. Res. Center, Univ. Wisconsin, Madison, Wis., 1971)*, pages 603–634. Academic Press, New York, 1971.

[55] P.D. Lax. *Hyperbolic systems of conservation laws and the mathematical theory of shock waves*. Society for Industrial and Applied Mathematics, Philadelphia, Pa., 1973. Conference Board of the Mathematical Sciences Regional Conference Series in Applied Mathematics, No. 11.

[56] P. G. LeFloch. Entropy weak solutions to nonlinear hyperbolic systems under nonconservative form. *Communications in partial differential equations*, 13(6):669–727, 1988.

[57] P. G. LeFloch. Shock waves for nonlinear hyperbolic systems in nonconservative form. *Institute for Math. and its Appl., Minneapolis, preprint*, 593:1989, 1989.

[58] P. G. LeFloch and T.-P. Liu. Existence theory for nonlinear hyperbolic systems in nonconservative form. *Forum Math.*, 5:261–280, 1993.

[59] Philippe G. LeFloch and Siddhartha Mishra. Numerical methods with controlled dissipation for small-scale dependent shocks. *Acta Numerica*, 23:743–816, May 2014.

[60] Philippe G. LeFloch and Majid Mohammadian. Why many theories of shock waves are necessary: Kinetic functions, equivalent equations, and fourth-order models. *Journal of Computational Physics*, 227(8):4162–4189, apr 2008.

[61] R. J. LeVeque. *Finite volume methods for hyperbolic problems*. Cambridge Texts in Applied Mathematics. Cambridge University Press, Cambridge, 2002.

[62] J.-M. Masella, I. Faille, and T. Gallouët. On a rough godunov scheme. *Int. J. for Computational Fluid Dynamics*, 12(2):133–150, 1999.

[63] T. Morales, M. J. Castro Diaz, and C. Parés. Reliability of first order numerical schemes for solving shallow water system over abrupt topography. *Applied Mathematics and Computation*, 219(17):9012–9032, 2013.

[64] T. Morales de Luna, M. J. Castro Diaz, and C. Parés Madronal. A duality method for sediment transport based on a modified meyer-peter & müller model. *Journal of Scientific Computing*, 48(1-3):258–273, 2011.

[65] C. Parés. Numerical methods for nonconservative hyperbolic systems: a theoretical framework. *SIAM Journal on Numerical Analysis*, 44(1):300–321 (electronic), 2006.

[66] E. Pimentel-García, Manuel J. Castro, C. Chalons, T. Morales de Luna, and C. Parés. In-cell discontinuous reconstruction path-conservative methods for non conservative hyperbolic systems - second-order extension. *Journal of Computational Physics*, page 111152, mar 2022.

[67] Nils Henrik Risebro and Aslak Tveito. Front tracking applied to a nonstrictly hyperbolic system of conservation laws. *SIAM Journal on Scientific and Statistical Computing*, 12(6):1401–1419, nov 1991.

[68] P. L. Roe. Approximate Riemann solvers, parameter vectors, and difference schemes. *J. Comput. Phys.*, 43(2):357–372, 1981.

[69] J.B. Schijf and J.C. Schönfled. Theoretical considerations on the motion of salt and fresh water. IAHR, 1953.

[70] D. Serre. *Systems of conservation laws. 1*. Cambridge University Press, Cambridge, 1999. Hyperbolicity, entropies, shock waves, Translated from the 1996 French original by I. N. Sneddon.

[71] E. Tadmor. Numerical viscosity and the entropy condition for conservative difference schemes. *Mathematics of Computation*, 43(168):369–381, 1984.

[72] E. Tadmor. A minimum entropy principle in the gas dynamics equations. *Appl. Numer. Math.*, 2(3-5):211–219, 1986.

[73] E. Tadmor. The numerical viscosity of entropy stable schemes for systems of conservation laws. i. *Mathematics of Computation*, 49(179):91–103, 1987.

[74] E. Tadmor. Entropy stability theory for difference approximations of nonlinear conservation laws and related time-dependent problems. *Acta Numerica*, 12(1):451–512, 2003.

[75] E Tadmor. Entropy stable schemes. *Handbook of Numerical Methods for Hyperbolic Problems: Basic and Fundamental Issues, edited by R. Abgrall and C.-W. Shu (North-Holland, Elsevier, Amsterdam, 2017)*, 17:467–493, 2016.

[76] E. F. Toro. *Riemann solvers and numerical methods for fluid dynamics*. Springer-Verlag, Berlin, third edition, 1997. A practical introduction.

[77] E.F. Toro, M. Spruce, and W. Speares. Restoration of the contact surface in the hll-riemann solver. *Shock Waves*, 4(4):25–34, 1994.

[78] J. Von Neumann and R.D. Richtmyer. A method for the numerical calculation of hydrodynamic shocks. *Journal of applied physics*, 21(3):232–237, 1950.